

# **MODULAR FLIGHT DYNAMIC MODELLING OF ROTARY-WING AIRCRAFTS**

**PROJECT REPORT**

Submitted by

**CB.EN.U4AEE19031 – SURYA N**

**CB.EN.U4AEE19048 – RAMCHARAN V**

*In partial fulfillment of credits for the award of the degree of*

**BACHELOR OF TECHNOLOGY**

**IN**

**AEROSPACE ENGINEERING**

*Under the guidance of*

**Dr. Sakthivel Thangavel**

Assistant Professor



**AMRITA SCHOOL OF ENGINEERING, COIMBATORE  
AMRITA VISHWA VIDYAPEETHAM, COIMBATORE**

**JUNE 2023**

**AMRITA VISHWA VIDYAPEETHAM**  
**AMRITA SCHOOL OF ENGINEERING, COIMBATORE – 641112**

**BONAFIDE CERTIFICATE**

This is to certify that the thesis entitled "**MODULAR FLIGHT DYNAMIC MODELLING OF ROTARY-WING AIRCRAFTS**" submitted by **SURYA N** (CB.EN.U4AEE19031) and **RAMCHARAN V** (CB.EN.U4AEE19048) in partial fulfilment of requirements for the award of the degree of Bachelor of Technology in **AEROSPACE ENGINEERING**, is a bonafide record of the work carried out under my guidance and supervision at the Amrita School of Engineering, Amritanagar, Coimbatore.

(Signature)  
**Dr. Sakthivel Thangavel**  
Assistant Professor  
Department of Aerospace Engineering  
Amrita School of Engineering  
Amritanagar, Coimbatore

This project was evaluated by us on:

(Internal Examiner)

(External Examiner)

**AMRITA VISHWA VIDYAPEETHAM**  
**AMRITA SCHOOL OF ENGINEERING, COIMBATORE – 641112**  
**DEPARTMENT OF AEROSPACE ENGINEERING**  
**DECLARATION**

We, **Surya N** (CB.EN.U4AEE19031) and **Ramcharan V** (CB.EN.U4AEE19048) hereby declare that this project entitled, “**MODULAR FLIGHT DYNAMIC MODELLING OF ROTARY-WING AIRCRAFTS**”, is a record of original work done by us under the guidance of **Dr. Sakthivel Thangavel**, Assistant Professor, Department of Aerospace Engineering, Amrita School of Engineering, Coimbatore. This project work is submitted as a part of the requirements for the award of the degree of Bachelor of Technology in Aerospace Engineering. The work presented in this report has not been submitted to any other University or Institute for the award of any degree or diploma.

1. Surya N :
2. Ramcharan V :

Place: Coimbatore

Date:

**Dr. Sakthivel Thangavel**  
Assistant Professor  
Department of Aerospace Engineering  
Amrita School of Engineering  
Amritanagar, Coimbatore

**Dr. V.Sivakumar**  
Professor and Chairperson  
Department of Aerospace Engineering  
Amrita School of Engineering  
Amritanagar, Coimbatore

## **Abstract**

Flight dynamic models are crucial for the process of aircraft design, load prediction, real-time simulation etc. A generic flight dynamic program for rotorcrafts that is modular in its architecture is a challenging yet rewarding task. Such a model enables designers to test different configurations and predict the impact of individual design parameters on the overall performance of the rotorcraft. This study aims to create a designer-friendly, generic, and modular flight dynamic model for rotorcrafts. The model incorporates a blade element approach with the quasi-steady theory to estimate the aerodynamic loads on the rotors. Additionally, a simple quasi-steady theory is employed for other components of the rotorcraft. Uniform, Drees, and Pitt-Peters dynamic inflow models are utilized to capture the rotor inflow dynamics. Generalized trim strategy for conventional and coaxial vehicle configurations is presented. The trim results for conventional vehicle configuration are validated with existing literature. This work presents a foundational and robust flight dynamic model for rotorcraft design and simulation, offering a versatile framework to explore various configurations. While substantial effort has been dedicated to its development, more research and refinement are essential for maximizing its potential. Through this solid groundwork, designers can now harness the model's capabilities to explore a wide range of rotorcraft configurations.

## Acknowledgement

We express our sincere gratitude to our project supervisors, Dr. Sakthivel Thangavel and Dr. Rajesh Senthil Kumar T, Department of Aerospace Engineering for their patient guidance and sincere efforts. They motivated us to work hard and inspired us to give our best. Their sincerity, perseverance and thoroughness have been invaluable to the work we present in this report. We thank all of our teachers at Amrita Vishwa Vidyapeetham for a great learning experience.

I, Surya N, would like to thank my parents Hema and Neelakandan and my sister Soundariya for their unconditional love, care and support. I also express my special gratitude to Dr. Balajee, Dr. V Laxman, and Dr. Nandu Gopan for the enlightening conversations, subject oriented, personal and philosophical. I thank my teammate and dear friend Ram, whose support, help and motivation I constantly seek. I thank all the brothers and sisters of my class. Priya, Suraj, Abhishek and Koushik deserve special mentioning for helping me with almost everything and any time. I thank my juniors for their support and pride. They will always remain dear to me.

I, Ramcharan V, would like to thank my father Viswanathan and my sisters Sridevi and Gowri for their love, prayers, caring and sacrifices for educating and preparing me for my future. I would like to appreciate all the faculty for their patience and support. I thank my teammate, Surya, for his positivity and guidance which helped me work in a team and bring out desired results. Also I express my special mention for my well wisher Snega and all my friends, thank you for your understanding and encouragement in my many moments of crises. I cannot list all names here, but you are always on my mind.

# Contents

<b>1</b>	<b>Introduction</b>	<b>1</b>
1.1	Definition and History . . . . .	1
1.2	Necessity and Utility of a Flight Dynamic Model . . . . .	2
1.3	Objectives . . . . .	2
<b>2</b>	<b>Literature survey</b>	<b>4</b>
2.1	Rotor Mathematical Modelling . . . . .	4
2.1.1	Sectional Aerodynamics . . . . .	4
2.1.2	Structural Modelling . . . . .	5
2.1.3	Inflow Modelling . . . . .	5
2.2	Fuselage and Stabilizers . . . . .	6
2.3	Existing Rotorcraft Flight Dynamic Models . . . . .	6
<b>3</b>	<b>Flight Dynamic Modelling</b>	<b>10</b>
3.1	Assumptions and Simplifications . . . . .	10
3.2	Reference Frames . . . . .	11
3.3	Velocity and Acceleration . . . . .	12
3.4	Rotor Model . . . . .	13
3.4.1	Sectional Loads . . . . .	13
3.4.2	Structural Modelling . . . . .	14
3.4.3	Inflow Modelling . . . . .	15
3.5	Fuselage Model . . . . .	17
3.6	Stabilizer Model . . . . .	18
3.7	Flight Dynamic Equation . . . . .	18
3.7.1	Equations of Motion . . . . .	18
3.7.2	Kinematic Relations . . . . .	19
<b>4</b>	<b>Construction of the Program</b>	<b>23</b>
4.1	Software used . . . . .	23
4.1.1	About the software . . . . .	23
4.2	Program Strategy . . . . .	24
4.3	Log Files . . . . .	25
4.4	Code Workflow . . . . .	25
4.4.1	Rotor loads . . . . .	25
4.4.2	Non-Rotating Component Loads . . . . .	27
4.4.3	Trim Analysis . . . . .	27

<b>5</b>	<b>Solution Methodology</b>	<b>30</b>
5.1	Mathematical Formulation for Trim . . . . .	30
5.2	Generalized Trim Procedure . . . . .	31
<b>6</b>	<b>Results</b>	<b>34</b>
6.1	Inflow for Conventional Configuration . . . . .	34
6.2	Flap for Conventional Configuration . . . . .	35
6.2.1	Observations . . . . .	35
6.3	Trim for Conventional Helicopter Configuration . . . . .	37
6.3.1	Observations . . . . .	37
6.3.2	Conventional Configuration Data . . . . .	38
6.4	Trim for Coaxial Configuration . . . . .	41
6.4.1	Coaxial Configuration Data . . . . .	42
<b>7</b>	<b>Conclusion</b>	<b>43</b>
<b>8</b>	<b>Future Scope</b>	<b>44</b>

# List of Figures

1.1	Helicopter Configurations . . . . .	3
2.1	Coordinate System of Helicopter . . . . .	8
2.2	Blade Reference Frames . . . . .	9
3.1	Velocity in Earth Fixed Frame . . . . .	21
3.2	Relation between Earth Fixed and Body Fixed Frames . . . . .	21
3.3	Parent - Child Reference Frame . . . . .	22
3.4	Idealized Rotor Blade in Flap Motion . . . . .	22
4.1	Non-rotating components load calculation . . . . .	28
4.2	Rotor load calculation . . . . .	28
4.3	Trim calculation . . . . .	29
5.1	Generalized Trim Procedure . . . . .	33
6.1	Inflow results for Conventional Configuration . . . . .	34
6.2	Flap Convergence . . . . .	36
6.3	Trim results for Conventional Configuration . . . . .	41

## List of Tables

1	Convergence study for Gaussian quadrature . . . . .	27
2	Conventional Configuration for Trim Analysis . . . . .	38
3	Trim Results for Conventional Configuration . . . . .	39
4	Coaxial Trim for $\mu=0$ (Hover) . . . . .	41
5	Coaxial Configuration for Trim Analysis . . . . .	42

## Symbols

$a$	lift curve slope of airfoil section of blade
$a_t$	lift curve slope of stabiliser
$a_t$	lift curve slope of tail Angle
$C_T$	rotor thrust coefficient
$C_{M_x}$	rotor aerodynamic rolling moment coefficient
$C_{M_y}$	rotor aerodynamic pitching moment coefficient
$c$	chord of rotor blade(m)
$c_d$	drag coefficient of an airfoil
$c_{dt}$	drag coefficient of stabiliser
$c_{dvt}$	drag coefficient of tail
$c_t$	chord of stabiliser(m)
$c_m$	pitching moment coefficient of an airfoil
$c_{m_t}$	pitching moment coefficient of stabiliser
$c_{m_t}$	pitching moment coefficient of tail
$c_t$	chord of tail
$\bar{D}$	sectional drag force of blade element
$e$	main rotor blade hinge offset(m)
$g$	gravitational acceleration( $m/s^2$ )
$I_b$	second mass moment of inertia of the blade( $kg.m^2$ )
$I_{xx}, I_{yy}, I_{zz}, I_{xz}$	mass moment of inertia of rotorcraft( $kg.m^2$ )
$k_\beta$	equivalent hinge flap stiffness
$L, M, N$	net moments at rotorcraft CG about x, y and z axes.
$m_r$	mass of the rotorcraft
$RX_h, RY_h, RZ_h$	rotor hub position from CG respectively
$RX_t, RY_t, RZ_t$	stabiliser position from CG
$s_f$	fuselage equivalent flat plate area
$s_t$	surface area of stabiliser

$s_t$	surface area of tail
$t$	time
$U$	resultant flow velocity on the airfoil section
$U_P$	normal component of airfoil net velocity
$U_T$	tangential component of airfoil net velocity
$\alpha$	incident angle
$\alpha_{t-i}$	initial setting angle of stabiliser
$\alpha_{t-i}$	initial setting angle of stabiliser
$\beta_k$	flap angle of $k^{th}$ blade
$\chi$	wake skew angle
$\lambda$	inflow ratio
$\lambda_D$	inflow ratio from Drees inflow model
$\lambda_{DI}$	inflow ratio from Dynamic inflow model
$\lambda_{UI}$	inflow ratio from uniform inflow
$\lambda_0$	mean inflow ratio
$\lambda_{1c}, \lambda_{1s}$	lateral / longitudinal inflow ratio
$\mu$	advance ratio
$\Omega$	rotor angular velocity
$\omega_{rf}$	rotor blade rotating flap frequency
$\Psi$	yaw attitude
$\psi_k$	azimuth angle of $k^{th}$ blade
$\Phi$	roll attitude
$\phi$	local induced angle of attack of a blade element
$\phi_t$	local induced angle of attack of stabiliser
$\phi_t$	local induced angle of attack of tail
$\theta$	pitch attitude
$\theta_i$	pitch input
$\theta_{eff}$	local effective angle of attack of blade element

$\theta_{tr}$	tail rotor collective pitch angle
$\theta_{tw}$	blade twist per unit length
$\theta_0$	collective pitch input
$\theta_{1c}$	lateral cyclic pitch input
$\theta_{1s}$	longitudinal cyclic pitch input
<i>Subscript – 0</i>	parent frame
<i>Subscript – 1</i>	child frame
$T_{01}$	DCM for parent to child frame transformation

## Abbreviations

<i>BET</i>	Blade Element Theory
<i>VTOL</i>	Vertical Take-Off and Landing
<i>VSTOL</i>	Vertical and Short Take-Off and Landing
<i>CFD</i>	Computational Fluid Dynamics
<i>FEM</i>	Finite Element Method
<i>CG</i>	Centre of Gravity
<i>HFR</i>	Hub Fixed Rotating Frame
<i>HFNR</i>	Hub Fixed Non-Rotating Frame
<i>RD</i>	Rotation-Direction Frame
<i>PB</i>	Pitch Bearing Frame
<i>FH</i>	Flap Hinge Frame
<i>LH</i>	Lag Hinge Frame
<i>TH</i>	Torsion Hinge Frame
<i>SA</i>	Station Airfoil Frame
<i>LOS</i>	Lift Off-Set
<i>DCM</i>	Direction Cosine Matrix
<i>TR</i>	Tail Rotor

# 1. Introduction

## 1.1 Definition and History

Rotary wing aircrafts, or rotorcrafts, are air vehicles that generate lift (also propulsion and/or control) by the action of one or more rotors. This category includes the likes of helicopters, drones, and tiltrotors (convertiplanes) [1] [2]. The unique advantage of rotorcrafts over fixed-wing aircrafts is their ability to take-off and land vertically (VTOL), hover in place and fly in any direction. They also offer more flexibility in the terrain of operation as the take-off and landing do not require sophisticated infrastructure. Although the design of rotorcrafts only matured in the twentieth century, the concept of rotary wings can be traced back to the 15th century sketches of Leonardo da Vinci. With the advancements in materials, computation and the theory of rotors, rotorcraft designs and applications have become more creative and robust. Some of the various designs and configurations tried throughout the years for different applications are discussed below with notable examples.

- Igor Sikorsky constructed the VS-300 in the 20th century. It was the world's first practical helicopter, but it only flew for a few seconds [3].
- In 1962, the Boeing CH-47 Chinook, a tandem-rotor helicopter was constructed by Vertol. This arrangement offers the advantage of supporting more weight with shorter blades and decreased disc area. However the complexities in transmission and gear systems can cause significant issues [1].
- The XV-15 was Bell's second-generation high-speed tiltrotor designed in 1970s. High-speed VTOL/VSTOL aircraft play a significant role in reducing traffic congestion on the ground and in the air. Their drawbacks include higher parasitic drag and structural weight. The transition from the take-off to cruise mode or vice versa can cause stability issues [4].
- In 1972, Kamov Ka-25, a coaxial helicopter, was developed as an anti-submarine helicopter to the Soviet military. Coaxial helicopters work by mounting two rotors on one axis and rotating them in opposite directions. Since a net-zero torque is produced, the requirement of a tail rotor is eliminated. Their drawbacks include complexity in rotor hub and controls design[1].

There are several more configurations that serve various applications. Detailing all existing configurations is beyond the scope of this report. But the discussion thus far is sufficient to establish the versatility in the existing designs and the utility of a generic flight dynamic model in aiding the process of design, development, and analysis.

## **1.2 Necessity and Utility of a Flight Dynamic Model**

The design and development of modern rotorcrafts, or aircrafts in general, involve extensive simulation in every step of design. Although the individual components are analysed using CFD, FEM and/or experimentation before finalization of design, an integrated flight dynamic simulation is essential to confirm the applicability of the model for the design requirements. This requires the utility of a flight dynamic model capable of simulating the design configuration with the desired accuracy. The benefit of analysing the flight dynamic performance in the conceptual design phase is significant.

The need for a modular flight dynamic model can be established by stating the benefits of such a model. Modularity implies that each component (such as the individual rotors, fuselage, and stabilizers) is modelled separately. Also, each of the physical phenomena necessary to model the components must be treated in a generalized manner. This is to ensure that the model can simulate multiple configurations while also ensuring that it provides variable features based on the designer's requirement. This flexibility is especially useful when evaluating the performance of modifications of existing designs.

The analysis enables designers to test and optimise alternative design configurations for the required flight conditions and manoeuvres. The data from the simulations can be used to make decisions regarding the capabilities and limitations of the aircraft. It also assists in identifying potential safety issues with the design, allowing designers to address these issues before the aircraft is built and flown. The other advantage is the elimination of the need for costly and time-consuming physical testing. These models can also be used as a pilot training tool where a realistic and interactive training environment is required.

## **1.3 Objectives**

Flight dynamic analysis includes prediction of trim states, stability characteristics, and open loop control response characteristics to pilot input and external disturbances. The objective of this work is to develop a flight dynamic program that can analyse and simulate generic rotorcraft configurations. The program is structured with independent modules to aid in the genericity and to make further development of the program easier.



(a) Chinook - Tandem



(b) Kamov ka-25 - Coaxial



(c) XV-15 - Tiltrotor

Figure 1.1: Helicopter Configurations

## 2. Literature survey

### 2.1 Rotor Mathematical Modelling

This chapter reviews the literature relevant to this project. This chapter consists of three sections. In the first section, rotor modelling is discussed in detail. The second section focuses on the modelling of the fuselage and stabilizer. In The final section, existing rotorcraft flight dynamic models are reviewed in detail.

#### 2.1.1 Sectional Aerodynamics

Evaluation of Aerodynamic loads on rotor blades are challenging due to unstable aerodynamic effects such as dynamic stall. During rotation, the advancing and retreating sides of the rotor blade undergo different aerodynamic phenomena. The advancing blades could suffer compressibility effects, transonic flow, and tip shock waves. Whereas The retreating blades could face reverse flow and stall effects. Cyclic pitch input and varying blade pre-twist causes the blade's angle of attack to vary continuously in both radial and azimuthal coordinates, causing continual variation in blade loads. The flow over the airfoil remains attached at low angles of attack whereas flow separation occurs at high angles of attack. This can result in dynamic stalling in rotor blade sections.

Theodorsen [5] proposed a three degrees of freedom model for an oscillating airfoil using incompressible potential flow and Kutta condition. The unsteady effects involved were represented by Theodorsen's lift deficiency function  $C(k)$ . Theodorsen's model was improved by Greenberg [6][7] by superimposing a time-varying incoming velocity component over a steady component. Lowey [8] modified the lift deficiency function to include the effects of inflow, number of blades and the ratio of oscillatory to rotational frequency. It should be noted that the theories discussed above ignore compressibility, viscosity and dynamic stall effects.

In order to accurately model the aerodynamics of rotating blades, including the dynamic stall effects is crucial. Originally, dynamic stall models were developed from experimental wind tunnel data of airfoil undergoing pitching and plunging motion. One of the most notable dynamic stall models includes the ONERA model developed by Petot et al [9]. Petot later extended his model by introducing new coefficients based on experimental data and other considerations. Laxman et al [10] proposed a modified ONERA model by representing the attached flow model by a second order differential equation. Several CFD models were also developed to predict the

aerodynamic loads on rotors [11].

In quasi-steady aerodynamic model, the lift deficiency function is assumed to be unity. Therefore, this model does not include the unsteady wake effects. The dynamic stall effects are also ignored. But, this model offers a simplistic approach to modelling the aerodynamics of airfoils. A linear lift curve slope can be implemented easily into the model to further simplify the analysis.

### 2.1.2 Structural Modelling

Rotor blade is generally modelled as a long slender beam undergoing flap, lag, torsion, and axial deformations. A detailed review of rotor blade structural modelling can be found in Kunz et al [12]. In late twentieth century, systematic formulations were developed using the theory of elasticity for rotor blades undergoing elastic deformation in flap, lag, torsion, and axial modes. An elastic hingeless blade is idealized as an equivalent rigid hinged blade as shown in fig 3.4. A root spring is added at the hinge in order to match the natural frequency of the rigid blade with the fundamental mode of the elastic blade. In the current study, the rotor blade is modelled as an equivalent rigid hinged blade undergoing flapping motion.

### 2.1.3 Inflow Modelling

The interaction between the rotor blades and the surrounding airflow is considered by the inflow model. The flow field that the rotating blades produce alters the direction of the entering airflow and the blades' angle of attack. The performance of the rotor system is impacted by the induced inflow as it affects the lift and drag forces exerted on the blades. Thus, the choice of inflow model is crucial to the accuracy of the results.

Inflow models are classified into time invariant and time varying (dynamic) inflow models. Time invariant inflow models essentially assume that the change in rotor thrust, and the associated inflow change occur instantaneously. But in reality, there exists a delay in time between the change in rotor thrust and the associated change in inflow. It is observed that the choice of inflow model strongly influences the lateral cyclic pitch and the roll attitude. It is also observed that the collective mode was largely unaffected while the longitudinal cyclic and the pitch attitude were affected to a small extend [13].

A review of various inflow models was presented in Chen et al[14] and Krothapalli et al[15]. Initially, the theory of uniform inflow was developed based on momentum

theory with the assumption that inflow through the rotor disc is uniform across the disc. Later, non-uniform inflow was modelled by combining momentum theory and blade element theory as a function of both radial and azimuthal location. Glauert proposed a first harmonic non-uniform inflow model that included a longitudinal variation of induced inflow velocity. This model predicted an upwash at the leading edge of the rotor disc and an increase in induced velocity at the trailing edge of the rotor disc [1]. The model was further refined by Coleman et al [16] and Mangler and Squire [17] to a Fourier series type expression. Later, Drees [14] obtained expressions for the first harmonic constants in terms of advance ratio and wake skew angle.

Dynamic inflow models include the time delay effects of the rotor blades' shifting pitch angles on the induced inflow velocity. Peters [18] states that dynamic inflow models possess two key characteristic features.

- They are mathematical models that predict inflow as a function of time, radial and azimuthal position for a given time history of loads.
- They are written as a system of ordinary differential equations.

Using the potential functions of Mangler and Squire, Pitt developed a closed-form representation of the  $[L]$  and  $[M]$  matrices that would connect the inflow equations and determine the temporal delays [15].

## 2.2 Fuselage and Stabilizers

The effect of rotor wake interactions on the fuselage is complex to model. A simplistic model for fuselage is obtained by predicting the drag produced as a function of equivalent fuselage flat plate area as obtained from wind tunnel experiments conducted by Wilson et al [19]. The rotor downwash also affects the stabilizers based on the configuration. In simple flight dynamic models, the rotor wake interactions with other components are ignored [13].

## 2.3 Existing Rotorcraft Flight Dynamic Models

A thorough investigation of existing literature on the modelling of rotary wing aircrafts is essential before further proceedings. A brief summary of some of the existing models is discussed below.

OpenVSP [20] (Open Vehicle Sketch Pad), is an open-source geometry and analysis tool developed by NASA for the conceptual design of aircrafts. CAD models can be

imported or developed within the software. Various models are available for aerodynamic, structural, and propulsive analysis with variable fidelity. Two potential flow solvers: vortex panel and vortex lattice modes from VSPAero can be used as aerodynamic solvers. High-fidelity CFD meshes can also be exported for further analysis. OpenVSP is widely used to perform preliminary analysis before proceeding to higher-fidelity analysis options such as CFD.

The model developed by Sakthivel T [13] for the flight dynamic analysis of helicopters focuses on analyzing helicopter flight in steady maneuvers to obtain trim, stability and control characteristics and estimate handling quality parameters. Various inflow models were tried with flapping motion to analyze the effect of inflow model on the trim states. Quasi-steady and modified ONERA dynamic stall models were used for sectional loads. The results were validated successfully with flight test data for conventional helicopter configuration. In this model, the blades were treated as rigid, and lag and torsion effects were not included.

The model developed by Laxman V et al[21], for the power and trim estimation for sizing of conventional helicopters improved on the existing helicopter sizing and performance computer program (HESCOMP) by introducing Blade Element Theory (BET) and uniform/non-uniform inflow. It was concluded that the lateral cyclic pitch is better determined with non-uniform inflow than uniform inflow. Since the model was developed for rotor sizing, considers a rigid blade without any twist or sweep. Other models that included aeroelastic effects, dynamic inflow and dynamic stall effects were later developed by Laxman V for the conventional helicopter configuration.

The GTRSim (Generic Tiltrotor Simulator) flight dynamic model built by NASA [22] as a generalization of the Bell Helicopter Textron program developed specifically for XV-15 tiltrotor aircraft. Owing to computational time constraints, steady state aerodynamics with uniform inflow was used. Using further approximations, the computational time was brought down drastically. The results agree with the flight test data of XV-15 with the exclusion of maneuvers that can cause stall, compressibility effects etc.

GENHEL model [23] posed problems in the hover and high-speed flight conditions due to improper modelling of aerodynamic interference in that flight regime. HeliUM 2, an upgraded version of HeliUM was developed by the University of Maryland [24] to improve on GENHEL. HeliUM 2 includes a high-fidelity rotor model, a dynamic inflow wake model, flexible blades with coupled nonlinear flap, lag, and torsion dy-

namics with structural flexibility. Arbitrary and multirotor aircraft configurations can be simulated using this model. The blade, wing and fuselage aerodynamic loads are obtained from non-linear look up tables, which might not be accurate in all flight conditions.

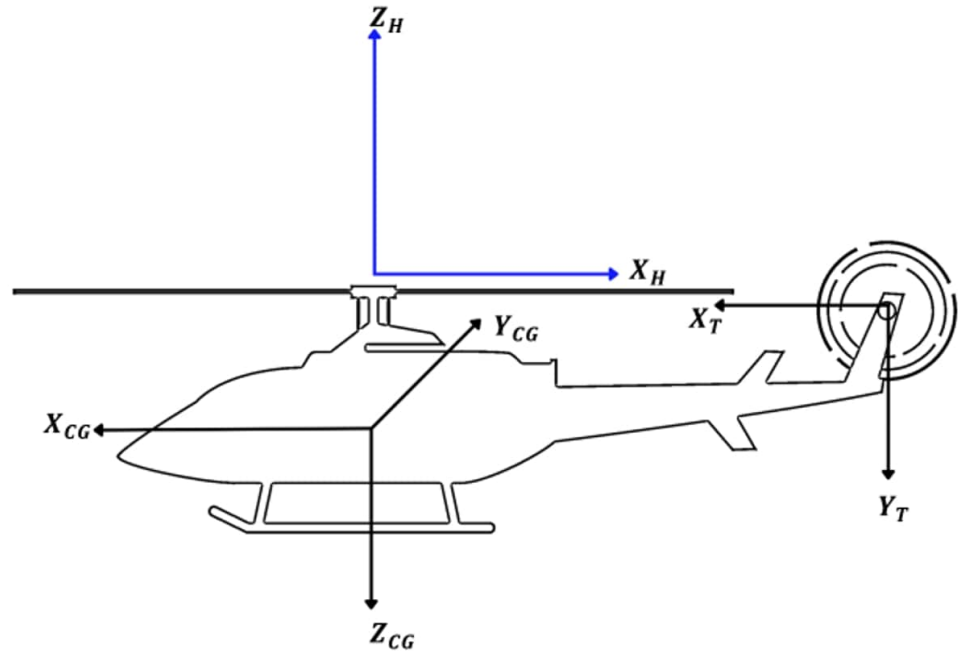


Figure 2.1: Coordinate System of Helicopter

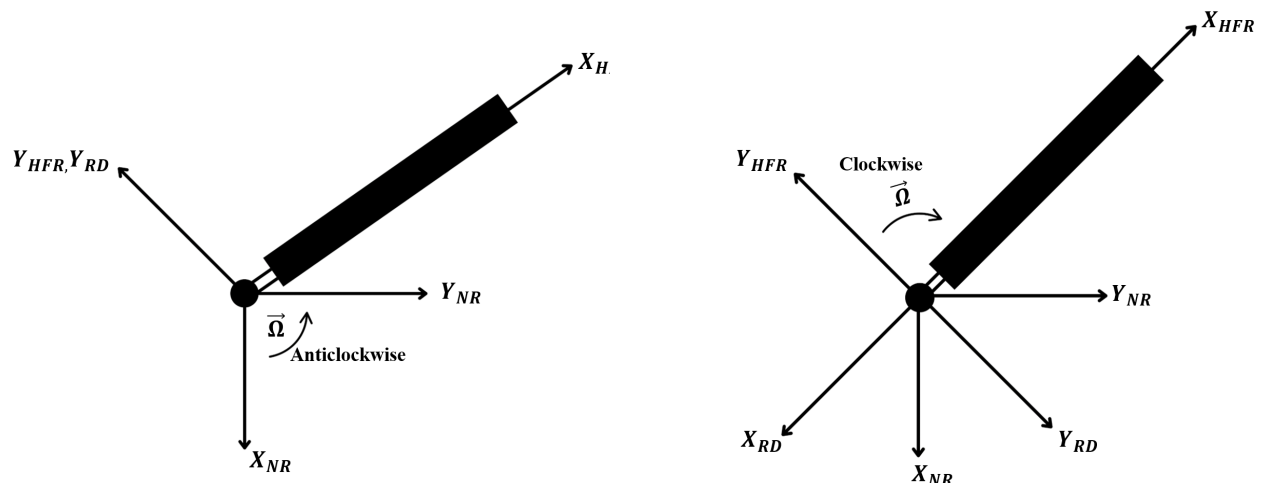
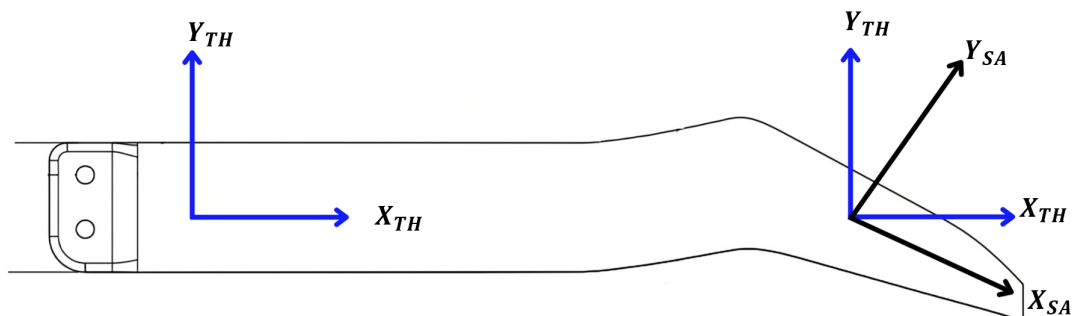
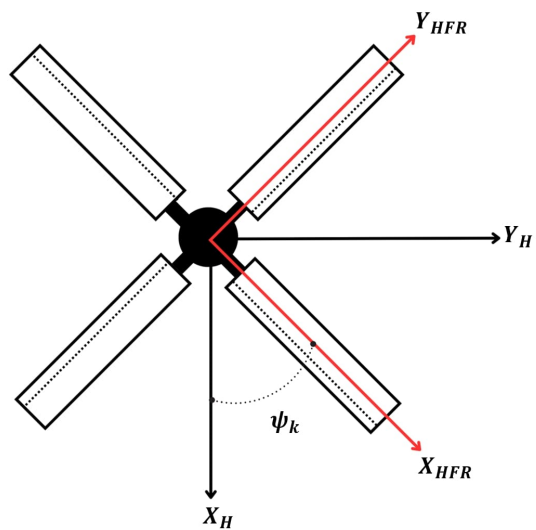


Figure 2.2: Blade Reference Frames

### 3. Flight Dynamic Modelling

The flight dynamic modelling of rotorcrafts involves developing comprehensive and independent models for rotor, stabilizer (empennage), and fuselage. Non-rotating components such as fuselage and stabilizers are also modelled for their aerodynamic loads. The flight dynamic equations and the kinematic relations are also included in this chapter. This chapter is divided into four sections. In the first section, the assumptions involved in the modelling along with the details of reference frames are described. The second section discusses the modelling of components. In the final section, the flight dynamic equations are described.

#### 3.1 Assumptions and Simplifications

- The fundamental assumption of BET is that the cross section of each blade behaves as a two-dimensional airfoil to generate aerodynamic loads.
- The rotor blades and other components are treated as rigid and equipped with an equivalent hinge offset with a root spring.
- Airfoil lift is assumed to vary linearly with angle of attack.
- Reverse flow, compressibility and stall effects are not considered.
- Only blade flapping is modelled. Torsion and lead-lag modes are not modelled.
- A constant angular velocity ( $\Omega$ ) is being maintained by the rotor system, so that the angular acceleration is said to be zero.
- The fuselage is treated as a flat plate producing drag force.
- The aerodynamic load acting on the blade is determined using quasi-steady state aerodynamic theory.
- The stabilizers are also modelled using the quasi-steady aerodynamic theory.
- Aerodynamic interaction between components is not modelled.

## 3.2 Reference Frames

The aerodynamic and structural modelling requires several reference frames to calculate and place the loads, angles and so on. The angle relationships between the reference frames are established by the means of direction cosine matrices. These reference frames are used to position and orient rotors, blades, hinges, airfoil sections etc. Required calculations are done in appropriate reference frames and transformed as and when required.

A number of reference frames are set up per component in order to model the physics involved in a consistent manner. All reference frames are right-handed. The vehicle's centre of gravity (CG) serves as the most fundamental reference frames. As will be discussed further, CG frame serves as the parent for the primary reference frames of all components. Since rotor modelling is crucial to our work, setting up reference frames for the rotors is a crucial task as well. In addition to this, the user should be able to set up the component position and orientation with respect to the CG frame freely. Fuselage and other non-rotating components such as the horizontal and vertical stabilizers are represented by one reference frame each. The reference frames defined for each component is elaborated below.

**Body Fixed CG frame (CG):** The CG frame is the base frame for all components. Since the CG frame is not oriented with respect to any other frame, the position and orientation of the CG frame can simply be assumed while entering the vehicle data in the input file. However, it is to be ensured that all position vectors and orientations of frames created using CG as parent follows the same convention.

**Hub-fixed non-rotating frame (HFNR):** One reference frame is set up at the rotor hub centre. The position is set up with respect to the CG reference frame. The orientation is set up via Euler angle. This frame serves as the parent for all the hub-fixed rotating frames.

**Hub-fixed rotating frame (HFR):** One reference frame is set up per blade to identify the azimuthal location of each blade throughout the calculations. The x axis of this frame is radially outward with the z axis parallel to the HFNR frame. This frame keeps track of the blade azimuth  $\Psi_k$ .

**Rotation-Direction frame (RD):** A reference frame is set up at the hub centre for each blade either parallel to the HFR frame or rotated 180 degrees about the z axis of HFR frame. This set up is done so that the code can handle rotor rotations in

both directions without changing the sign convention of the cyclic pitch input. This is mainly useful in the case of coaxial rotors. If the rotation is anticlockwise with respect to z axis, this frame remains parallel to the HFR frame. Whereas if the rotation is clockwise, the reference frame is rotated by 180 degrees so that the x axis points towards the hub instead of radially outward and the y axis of this frame points at the direction of motion of the blade.

**Pitch bearing frame (PB):** A reference frame is set up to provide cyclic pitch input  $\Theta_I$  for the blade. The position vector and orientation of this frame is set with respect to the RD frame. The frame rotates about its x axis to control the blade pitch. Since the x axis is flipped inward for the clockwise rotating rotor, the sign of the pitch input need not be changed.

**Flap hinge frame (FH):** This reference frame is created from PB with an angle  $\beta_k$  with respect to the y axis of PB frame. This frame is set with flap hinge offset as its position vector as calculated from PB.

**Lag hinge frame (LH) and Torsion hinge frame (TH):** The LH frame is oriented with an angle  $\varsigma$  with respect to the z axis of FH and TH is oriented with an angle  $\phi$  with respect to the x axis of LH. Currently, both of these frames are set with zero angles because the lag and torsion dynamics modules are yet to be developed. The reference frames are created at this time to readily support the future development of the code.

**Station airfoil frame (SA):** The SA is defined with respect to TH. The position vectors are set based on the required number of stations per blade. Any blade sweep read from the user input is imposed on this frame with respect to the z axis of TH frame.

### 3.3 Velocity and Acceleration

The net velocity and net acceleration are necessary to model the aerodynamics and dynamics of the blade respectively. Defined reference frames are utilized in the calculation of net velocity and acceleration. The standard relation to find net velocity of a child reference frame fig 3.3 is as follows:

$$\{X_1\} = T_{01} \{X_0\} \quad (3.3.1)$$

$$\vec{V}_{0,net} = T_{01} \vec{V}_{0,net} + T_{01} (\vec{w}_{0,net} t \times R_{01}) \quad (3.3.2)$$

Net acceleration of the child frame is obtained by differentiating this velocity rela-

tion. In doing so, any rate of change of position vectors is ignored. This means that the positions of the reference frames do not change with respect to their parent. This is a noteworthy simplification as the position vector of each component reference frame defined directly from CG should suffer a rate of change due to change in CG position due to fuel depletion. But this effect is ignored in the current analysis. The net acceleration is estimated as follows:

$$\vec{a}_{0,net} = T_{01}\vec{a}_{0,net} + T_{01}(\vec{w}_{0,net} \times \dot{\vec{R}}_{01}) + T_{01}(\dot{\vec{w}}_{0,net} \times R_{01}) + \dot{T}_{01}(\vec{w}_{0,net} \times R_{01}) \quad (3.3.3)$$

$$\dot{\vec{R}}_{01} = 0 \quad (3.3.4)$$

$$\vec{a}_{0,net} = T_{01}\vec{a}_{0,net} + T_{01}(\vec{w}_{0,net} \times R_{01}) + \dot{T}_{01}(\vec{w}_{0,net} \times R_{01}) \quad (3.3.5)$$

## 3.4 Rotor Model

Rotor modelling can be further segregated into aerodynamic, structural and inflow modelling. In the current work, structural modelling involves flap dynamics. Sectional aerodynamics is modelled using quasi-steady aerodynamic theory. Inflow modelling involves uniform, non-uniform, and dynamic inflow models.

### 3.4.1 Sectional Loads

Sectional loads are modelled using quasi-steady theory. Although the theory involves several simplifying assumptions, its simplicity makes it an attractive option in flight dynamic modelling.

#### 3.4.1.1 Quasi-steady Theory

The quasi-steady aerodynamic theory, involving the quasi-steady assumption, is a simplified theory that states that the aerodynamic forces on any object can be treated as constant with time for quasi-steady flow. A quasi-steady flow is where the flow properties are changing too slowly for their rates of change to produce significant contributions to the calculations. In this method, aerodynamic lift is evaluated based on the instantaneous angle of attack at every blade cross section [1]. This helps in making simple predictions without considering complex unsteady effects. Although the theory does not capture unsteady effects, it is a viable tool to provide quick approximations of aerodynamic loads.

### 3.4.1.2 Blade Element Theory

BET forms the foundation of all aerodynamic analyses of rotors. The relationship between rotor performance and the blade and airfoil design parameters is established with use of BET. Although the theory was proposed by Froude in 1878, Stefan Drzewiecki was the first to put it to serious use in early twentieth century [1]. BET involves the following major assumptions:

- It treats each cross section of a blade as an airfoil that produces lift, drag and pitching moment.
- The effect of rotor wake is entirely attributed to the induced inflow angle at each cross section. Hence, an estimate of induced inflow velocity at each station is required.
- Plane of rotation of blade is perpendicular to the shaft axis (z-axis of HFNR).

In BET, sectional aerodynamic forces and moments are obtained as functions of radial and azimuthal location, and in terms of local induced inflow, local angle of attack and other local properties. The obtained functions are then integrated along the blade radius using the Gauss-Quadrature algorithm to obtain the net aerodynamic loads on the blade. Likewise, loads from each blade is vectorially added to obtain the net loads at the rotor hub.

### 3.4.2 Structural Modelling

Flap response refers to the behaviour of the rotor blades in response to changes in the control inputs, such as changes in collective pitch or cyclic pitch. Blade flapping is caused due to variation in lift forces. Flap response is an important consideration in the design and operation of rotary wing aircraft, as it affects the aircraft's performance characteristics. In forward flight, the blade flapping and pitch input influence the hub loads strongly [1]. The flap equation is obtained by applying y-moment equilibrium relation about the flap hinge (FH frame). This equation contains contributions from the inertial and aerodynamic loads as well as the restraint (spring) moment at the hinge.

$$M_{Inertial} + k_\beta \ddot{\beta} = M_{aerodynamic} \quad (3.4.1)$$

$$f(\ddot{\beta}, \beta) = 0 \quad (3.4.2)$$

$$\omega_n = \bar{\omega}_{RF} = \frac{\omega_{RF}}{\Omega} = \sqrt{1 + \frac{3}{2} \frac{\bar{e}}{1 - \bar{e}} + \frac{k_\beta}{I_b \Omega^2}} \quad (3.4.3)$$

Here,  $k_\beta$  is the equivalent hinge flap stiffness. This second order equation is converted into two first order differential equations and solved using the 4th order Runge-Kutta method to obtain the flap response in time domain for each blade separately.

### 3.4.3 Inflow Modelling

In this work, the load and inflow calculations are handled separately. Therefore, the complexity of either of the models can be specified depending on the application. This modularity is required to provide variable fidelity options to the user.

Inflow modelling in rotors is divided into two types, namely:

- Time invariant inflow

Uniform

Non-uniform (Drees inflow)

- Time varying inflow

Dynamic inflow (Pitt-Peters model)

The choice of inflow model is crucial to the accuracy of the results. As per the results produced by Sakthivel T[13], it was observed that the choice of inflow model strongly influences the lateral cyclic pitch and the roll attitude. It was also observed that the collective mode was largely unaffected while the longitudinal cyclic and the pitch attitude were affected to a small extend. Therefore, three models are included in this work to achieve variability in terms of computational effort and accuracy.

#### 3.4.3.1 Uniform Inflow

In uniform inflow, the inflow to the rotor disk is assumed to have a constant velocity across the entire rotor disk area. Hence, the predicted inflow value will not vary with time or radial and azimuthal position. In reality, the inflow through a rotor disc varies with time, radial or azimuthal position. While the model does not produce highly accurate results, it is used in the rotor aerodynamic modelling as it involves less computational effort. Moreover, the uniform inflow model is often used as a basis for higher accuracy inflow models.

$$\lambda = \mu \tan \alpha + \lambda_i \quad (3.4.4)$$

$$\lambda = \mu \tan \alpha + \frac{C_T}{2\sqrt{\mu^2 + (\mu \tan \alpha + \lambda_i)^2}} \quad (3.4.5)$$

$$\lambda = \mu \tan \alpha + \frac{C_T}{2\sqrt{\mu^2 + \lambda}} \quad (3.4.6)$$

### 3.4.3.2 Drees inflow

Drees inflow is a non-uniform inflow model where the induced inflow velocity is treated as a function of radial and azimuthal position. This theory predicts different inflow values at different sections of the blade at different azimuthal positions. As discussed before, Drees derived closed form expression for the first harmonics of inflow in terms of wake skew angle  $\chi$  and advance ratio  $\mu$ . As this model captures more physics than the uniform inflow model, the results obtained are comparatively better.

$$\chi = \tan^{-1} \frac{\mu}{\lambda_{UI}} \quad (3.4.7)$$

$$k_x = -2\mu \quad (3.4.8)$$

$$k_y = \frac{4}{3} [ (1 - 1.8\mu^2) \csc \chi - \cot \chi ] \quad (3.4.9)$$

$$\lambda_{1s} = \lambda_i k_x \quad (3.4.10)$$

$$\lambda_{1c} = \lambda_i k_y \quad (3.4.11)$$

$$\lambda_0 = \mu \tan \alpha_i + \lambda_i \quad (3.4.12)$$

$$\lambda_D(\bar{r}, \psi) = \lambda_0 + \lambda_{1s}\bar{r} \sin \psi + \lambda_{1c}\bar{r} \cos \psi \quad (3.4.13)$$

There is periodic variation in the relative position of the blade and the wake-vortices shed by it. This periodicity causes strong variations in the wake-induced velocity and as an effect, in the blade loading [1]. There is also a lag in time between the variation in inflow and the corresponding drop in the lift for time-varying cyclic inputs. Although this theory models this phenomenon, it fails to capture the time delay in interactions between the induced inflow velocity and the resulting loads at the blade. This model offers lesser computational requirement than any of the dynamic inflow models while also providing a better estimate than the uniform inflow model.

### 3.4.3.3 Dynamic Inflow

In this work, we use Peters and Pitt's dynamic inflow model [25]. It models the interactions between induced inflow and load response including the time delay between the variation in inflow and the corresponding change in load as a system of

three ODEs. Pitt developed a closed-form representation of the [L] and [M] matrices that would connect the inflow equations and determine the temporal delays using the potential functions of Mangler and Squire[17].

$$\lambda_{DI}(\bar{r}, \psi) = \mu \tan \alpha_i + \lambda_i + \lambda_{1s} \bar{r} \sin \psi + \lambda_{1c} \bar{r} \cos \psi \quad (3.4.14)$$

$$[M] \begin{Bmatrix} \dot{\lambda}_1 \\ \dot{\lambda}_{1s} \\ \dot{\lambda}_{1c} \end{Bmatrix} + [V][L]^{-1} \begin{Bmatrix} \lambda_1 \\ \lambda_{1s} \\ \lambda_{1c} \end{Bmatrix} = \begin{Bmatrix} C_T \\ C_{M_x} \\ C_{M_y} \end{Bmatrix} \quad (3.4.15)$$

L matrix,

$$L = \begin{bmatrix} \frac{1}{2} & 0 & \frac{15\pi}{64} \tan \frac{\chi}{2} \\ 0 & \frac{-4}{1+\cos\chi} & 0 \\ \frac{15\pi}{64} \tan \frac{\chi}{2} & 0 & \frac{-4\cos\chi}{1+\cos\chi} \end{bmatrix} \quad (3.4.16)$$

Velocity matrix,

$$V = \begin{bmatrix} V_T & 0 & 0 \\ 0 & V_R & 0 \\ 0 & 0 & V_R \end{bmatrix} \quad (3.4.17)$$

$$V_T = \sqrt{\mu^2 + \lambda_{UI}^2} V_R = \frac{\mu^2 + \lambda_{UI}(\lambda_{UI} + \lambda_i)}{\sqrt{\mu^2 + \lambda_{UI}^2}} \quad (3.4.18)$$

Apparent mass matrix,

$$[M] = \begin{bmatrix} \frac{8}{3\pi} & 0 & 0 \\ 0 & \frac{-16}{45\pi} & 0 \\ 0 & 0 & \frac{-16}{45\pi} \end{bmatrix} \quad (3.4.19)$$

### 3.5 Fuselage Model

In general, the fuselage is the aircraft's primary body, which holds the cockpit, passengers, cargo, and/or engine. It is often cylindrical or pod shaped. It is aerodynamically engineered to provide lift and stability to the helicopter during flight. Multiple fuselage configurations can also be analysed in the current work. Currently, the fuselage component is modelled only as a drag-producing body. Quasi-steady model is utilized to estimate this drag in terms of equivalent fuselage flat plate area. The estimated drag is then transferred to CG appropriately.

$$D_{heli} = \frac{1}{2} \rho a \mu^2 (\Omega R)^2 s_f \quad (3.5.1)$$

### 3.6 Stabilizer Model

The stabilizer/empennage is the aircraft's tail section, which usually contains the horizontal stabiliser and vertical fin. As the name suggests, stabilizers help in stabilizing the aircraft. The conventional horizontal and vertical stabilizers aid in pitch and yaw stability of the aircraft respectively. The quasi-steady model is utilized to evaluate the aerodynamic forces and moments. The estimated loads are then transferred to CG appropriately.

$$L = \frac{1}{2} \rho_a a s U^2 \alpha \quad (3.6.1)$$

$$D = \frac{1}{2} \rho_a s U^2 C_d \quad (3.6.2)$$

$$m = \frac{1}{2} \rho_a c s U^2 C_m \quad (3.6.3)$$

### 3.7 Flight Dynamic Equation

#### 3.7.1 Equations of Motion

The equations of motion for an aircraft in flight are a collection of differential equations that describe an aircraft's motion in terms of location, velocity, and acceleration. They are an expression of equilibrium relations that consider the weight, propulsion, and aerodynamic forces that affect the aircraft. The set of six second-order differential equations known as the six degrees of freedom equations of motion are derived from Newton's principles of motion. Force equations:

$$\dot{u} = -(wq - vr) + \frac{X}{m_h} - g \sin\theta \quad (3.7.1)$$

$$\dot{v} = -(ur - wp) + \frac{Y}{m_h} + g \cos\theta \sin\phi \quad (3.7.2)$$

$$\dot{w} = -(vp - uq) + \frac{Z}{m_h} + g \cos\theta \cos\phi \quad (3.7.3)$$

Moment equations:

$$I_{xx}\dot{p} = (I_{yy} - I_{zz})rq + I_{xz}(\dot{r} + pq) + L \quad (3.7.4)$$

$$I_{yy}\dot{q} = (I_{zz} - I_{xx})rp + I_{xz}(r^2 - p^2) + M \quad (3.7.5)$$

$$I_{zz}\dot{r} = (I_{xx} - I_{yy})pq + I_{xz}(\dot{p} - rq) + N \quad (3.7.6)$$

Here, it can be seen that both x and z moment equations contain  $\dot{p}$  and  $\dot{r}$ . Solving  $\dot{p}$  and  $\dot{r}$  yields:

$$\dot{p}(I_{xx}I_{zz} - I_{xz}^2) = q(rI_{zz}(I_{yy} - I_{zz}) - I_{xz}^2) + pI_{xz}(I_{xx} - I_{yy} + I_{zz}) + I_{zz}L + I_{xz}N \quad (3.7.7)$$

$$\dot{r}(I_{xx}I_{zz} - I_{xz}^2) = (q(rI_{xz}(I_{yy} - I_{zz} - I_{xz})) + p(I_{xx}(I_{xx} - I_{yy}) + I_{xz}^2)) + I_{xz}L + I_{xx}N \quad (3.7.8)$$

### 3.7.2 Kinematic Relations

Earth fixed (NED- north-east-down) frame and CG frame are utilized in developing the kinematic relations of both translational and rotational motions of the rotorcraft. The relation between the body angular rates with Euler angles and turn rate are given by the following relations:

$$p = \dot{\Phi} - \dot{\Psi} \sin \Theta \quad (3.7.9)$$

$$q = \dot{\Theta} \cos(\Phi) + \dot{\Psi} \cos \Theta \sin \Phi \quad (3.7.10)$$

$$r = -\dot{\Theta} \sin(\Phi) + \dot{\Psi} \cos \Theta \cos \Phi \quad (3.7.11)$$

$$\dot{\Phi} = p + q \sin \Phi \tan \Theta + r \cos \Phi \tan \Theta \quad (3.7.12)$$

$$\dot{\Theta} = q \cos \Phi - r \sin \Phi \quad (3.7.13)$$

$$\dot{\Psi} = q \frac{\sin \Phi}{\cos \Theta} + r \frac{\cos \Phi}{\cos \Theta} \quad (3.7.14)$$

The velocity components of the flight speed  $V_f$  in Earth fixed system:

$$\begin{bmatrix} u_{ea} \\ v_{ea} \\ w_{ea} \end{bmatrix} = \begin{bmatrix} V_f \cos \gamma_f \cos \chi_e \\ V_f \cos \gamma_f \sin \chi_e \\ V_f \sin \gamma_f \end{bmatrix} \quad (3.7.15)$$

The Euler angles correspond to the orientation of the rotorcraft with respect to Earth fixed coordinate system. The sequence of rotation is yaw  $\Psi$ , pitch  $\Theta$  and roll  $\phi$ .

$$\begin{bmatrix} X_1 \\ Y_1 \\ Z_1 \end{bmatrix} = \begin{bmatrix} \cos\Psi & \sin\Psi & 0 \\ -\sin\Psi & \cos\Psi & 0 \\ 0 & 0 & 1 \end{bmatrix} \begin{bmatrix} X_e \\ Y_e \\ Z_e \end{bmatrix} \quad (3.7.16)$$

$$\begin{bmatrix} X_2 \\ Y_2 \\ Z_2 \end{bmatrix} = \begin{bmatrix} \cos\Theta & 0 & -\sin\Theta \\ 0 & 1 & 0 \\ \sin\Theta & 0 & \cos\Theta \end{bmatrix} \begin{bmatrix} X_e \\ Y_e \\ Z_e \end{bmatrix} \quad (3.7.17)$$

$$\begin{bmatrix} X_b \\ Y_b \\ Z_b \end{bmatrix} = \begin{bmatrix} 1 & 0 & 0 \\ 0 & \cos\Phi & \sin\Phi \\ 0 & -\sin\Phi & \cos\Phi \end{bmatrix} \begin{bmatrix} X_e \\ Y_e \\ Z_e \end{bmatrix} \quad (3.7.18)$$

The rotations result in the final transformation of the form:

$$\begin{bmatrix} X_b \\ Y_b \\ Z_b \end{bmatrix} = \begin{bmatrix} 1 & 0 & 0 \\ 0 & \cos\Phi & \sin\Phi \\ 0 & -\sin\Phi & \cos\Phi \end{bmatrix} \begin{bmatrix} \cos\Theta & 0 & -\sin\Theta \\ 0 & 1 & 0 \\ \sin\Theta & 0 & \cos\Theta \end{bmatrix} \begin{bmatrix} \cos\Psi & \sin\Psi & 0 \\ -\sin\Psi & \cos\Psi & 0 \\ 0 & 0 & 1 \end{bmatrix} \begin{bmatrix} X_{ea} \\ Y_{ea} \\ Z_{ea} \end{bmatrix} \quad (3.7.19)$$

The vector transformation can also be expressed in a simplified manner using the flight track angle  $\chi_e$  as follows:

$$\chi_e = \chi - \psi = \chi - \Omega_f t \quad (3.7.20)$$

The angle of attack and sideslip angles can be expressed as follows:

$$u = V_f(\cos\Theta\cos\gamma_f\cos\chi_e - \sin\Theta\sin\gamma_f) \quad (3.7.21)$$

$$v = V_f(\cos\Phi\cos\gamma_f\sin\chi_e + \sin\Phi(\sin\Theta\cos\gamma_f\cos\chi_e + \cos\Theta\sin\gamma_f)) \quad (3.7.22)$$

$$w = V_f(-\sin\Phi\cos\gamma_f\sin\chi_e + \cos\Phi(\sin\Theta\cos\gamma_f\cos\chi_e + \cos\Theta\sin\gamma_f)) \quad (3.7.23)$$

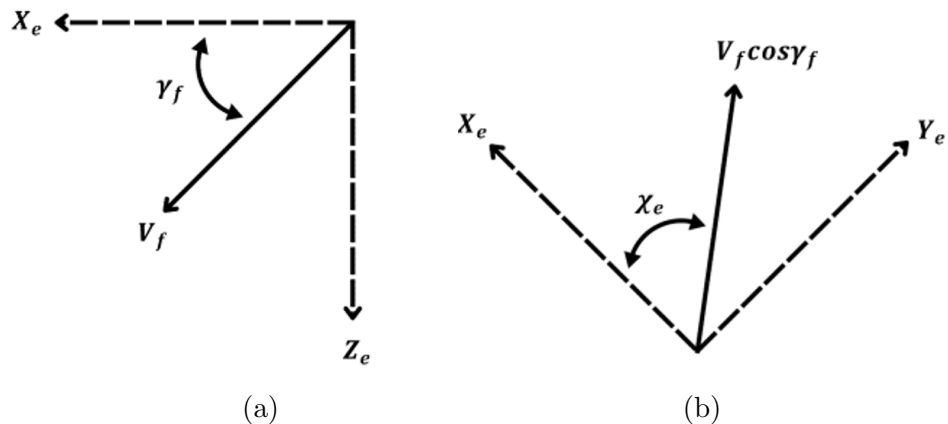


Figure 3.1: Velocity in Earth Fixed Frame

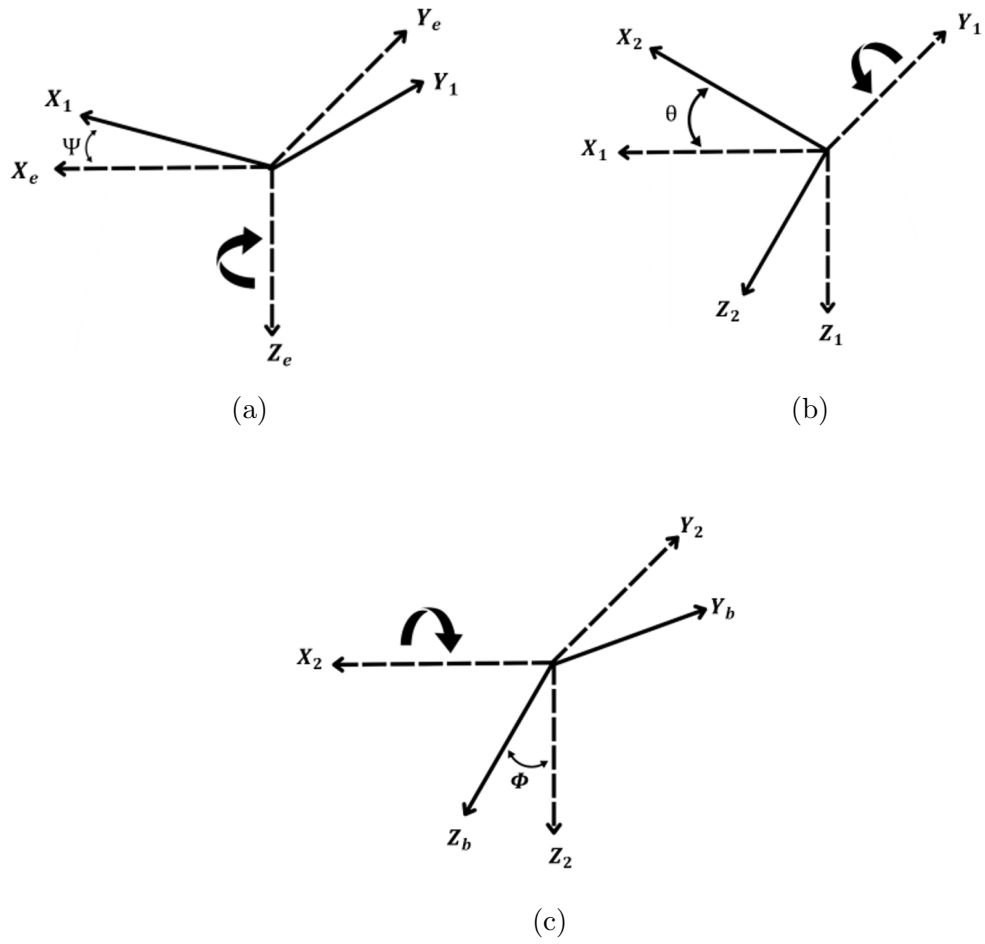


Figure 3.2: Relation between Earth Fixed and Body Fixed Frames

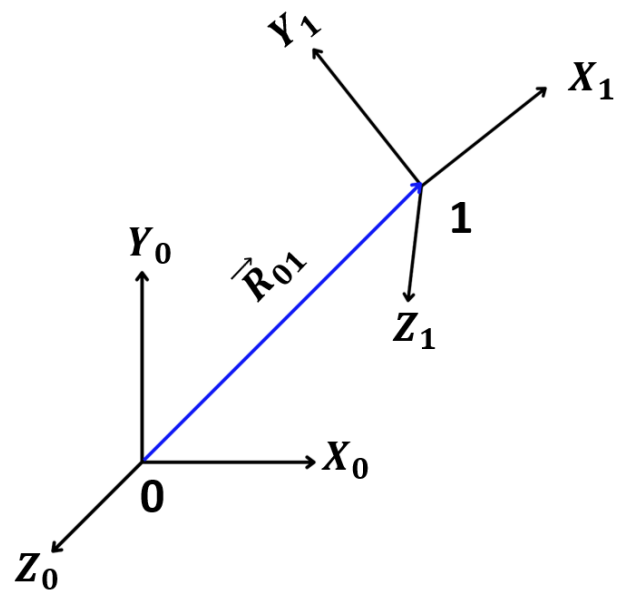


Figure 3.3: Parent - Child Reference Frame

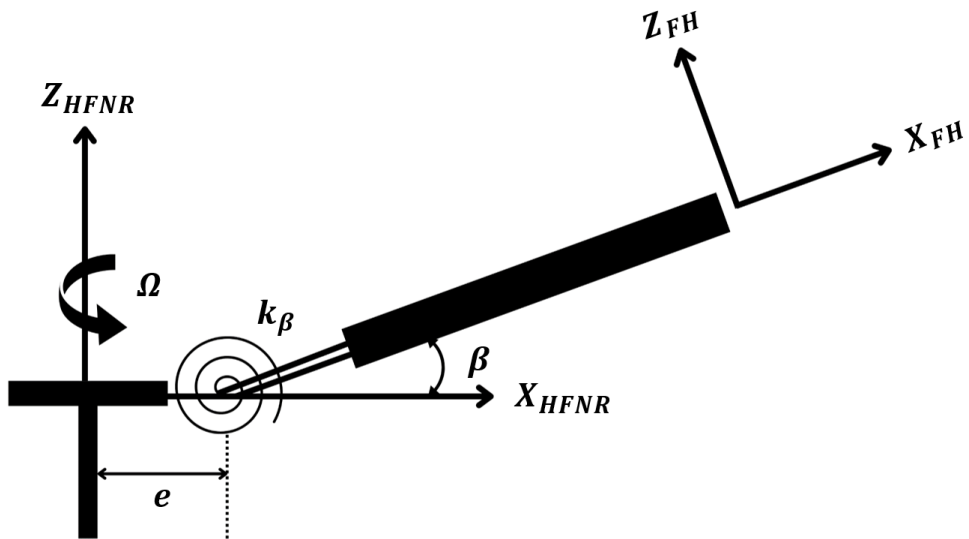


Figure 3.4: Idealized Rotor Blade in Flap Motion

## 4. Construction of the Program

Construction of a modular and generic program for the flight dynamic analysis of rotorcrafts is not a simple task. It requires proper selection of the programming language, supportive software, usage of libraries and so on. A detailed discussion of the procedure and workflow of the program is carried out in this chapter. This chapter consists of three sections. An overview of the programming language and other software tools is presented in the first section. The second section briefly discusses the code files, their dependencies and functionalities. The third section focuses on the workflow of essential load calculation modules.

### 4.1 Software used

It is relevant to briefly discuss about the software and libraries used in this work. The program is written and run in Python 3.10 with the help of PyCharm IDE. The program uses Microsoft Excel for the input file containing vehicle configuration data. Various Python libraries are also installed and used.

#### 4.1.1 About the software

Python is a general-purpose, high-level programming language with emphasis on simplicity and code readability. It is an open-source programming language/software. It is a multi-paradigm language in that it supports functional, object-oriented, and structured programming. It is one of the most popular programming languages in the world. Many standard mathematics and physics libraries are available open source. Python is chosen for this work based on the support to modularity, object-oriented programming, and simplicity of syntax. Python version 3.10 is used in this code. Microsoft Excel (MS Excel) is a popular spreadsheet software that performs data storage and analytics. Due to its ease of readability and use, the input file is chosen to be an MS Excel file. In addition to this, required Python libraries were also imported for specific utility as listed below.

- Numpy - Matrix manipulations.
- Sympy - Reference frames and direction cosine matrices.
- Math - Mathematical functions like square root.
- Pandas - Reading excel sheets and data manipulation.

## 4.2 Program Strategy

The vehicle configuration data is to be entered in the prescribed excel file in the prescribed format. The code reads the entered vehicle parameters, rotor data, other component data and the required initial conditions and stores it as attributes of relevant class objects systematically. All the required reference frames are created using the component data retrieved from input file. Further calculations are done based on the required analysis. Individual classes with required attributes are created for the rotors, fuselages, and stabilizers. Each component in the input file is created as an object of the appropriate class with all the attributes.

**Global File:** This file is used to store variables in a centralized fashion. This enables ease of access to the variables from any other module. This module hosts the component class definitions for rotors, fuselages, and stabilizers. It also hosts the class definitions for the atmospheric data class and the log text file formats for writing the relevant calculated values in other module

**Read Input File:** This file is used to read the component data from excel file and store as appropriate class objects in Global file.

**Atmosphere File:** This file hosts the function for the International Standard Atmosphere. This function is used to calculate, and assign required atmospheric data to the atmospheric data class in Global file.

**Reference Frames File:** This file hosts the functions that create and manipulate reference frames, perform vector operations such as velocity and acceleration calculations etc.

**Numerical Methods File:** This file hosts the functions that perform numerical calculations such as Newton-Raphson, Gauss-Quadrature, Linear interpolation etc.

**Inflow Model File:** This file hosts the functions for uniform, non-uniform, and dynamic inflow models.

**Aerodynamics File:** This file hosts the functions to estimate sectional loads, integrated hinge loads etc.

**Structural Model File:** This file hosts the functions for inertial load estimation, flap calculations etc.

**Rotor Loads File:** This file hosts the functions for estimating the net loads of all rotating components after inflow and/or flap convergence and transfer them to CG frame.

**Trim Analysis File:** This file hosts the logic for the trim routine for different configurations and the transformations from Earth fixed frame to CG frame for velocities. It also hosts the flight dynamic equations required for trim analysis.

### 4.3 Log Files

As we have discussed so far, the analysis with rotors involves extensive calculations. This also means that plenty of data is available from every calculation. Thus, creating log files of these data can be very useful for analysis after the code has terminated successfully. This also allows faster debugging of the code as any problem can be traced after the code has failed without having to re-run it multiple times. In addition to these benefits, logging the calculated data creates prospects of improvement like an interactive GUI with real-time plotting or analysis features.

Based on the context of data, five log files are required. Inflow file stores information relevant to inflow calculations such as azimuthal location, instantaneous component thrust, moments, their coefficients, and the computed inflow values. Flap file stores the azimuthal location, blade number, flap angle, its first and second derivative value. Section data file stores all data relevant to station calculations such as the total inflow value, station net velocity, cyclic pitch, induced and effective angle of attack, section loads etc. Components data file stores the net component loads at their primary reference frames (such as HFNR for the rotors) after successful computation of loads. Lastly, the trim file stores the initial input trim conditions, CG velocities, accelerations at each Newton-Raphson iterations, the time taken for the iteration, the final trim result etc.

### 4.4 Code Workflow

#### 4.4.1 Rotor loads

Rotor load calculation, as was discussed earlier, is the most important aspect of this analysis. Thus, utmost care must be exercised in determining the numerical scheme used for radial integration of obtained sectional loads. Initially, Simpson's method was employed to integrate sectional loads. In order to produce accurate results, this method required a large number of stations for higher forward speeds. This effect can be attributed to the fact that Simpson's method uses quadratic interpolation between the points. The load distribution along the blade radius gets more complicated with increasing flight speed. But runtime and computation effort increase with increasing number of stations. Therefore, the Gaussian quadrature algorithm was set for integrating the sectional loads in an attempt to reduce the number of

stations. An investigative study to find the minimum number of stations required to compute the loads with reasonable accuracy was conducted. Table 1 displays the values of blade loads for 10, 20, 30 and 40 stations respectively. From this, it can be concluded that for 20 stations, accurate results can be obtained. But, for 20 point Gaussian quadrature method with twenty stations, the runtime still remains high. Therefore, the preliminary calculations whose results are displayed in this report are done with ten stations and 10-point Gaussian quadrature.

A broad step-by-step procedure involved in the calculation of rotor loads is presented below table 1.

- Inflow calculation is performed using the inflow model with the initial inflow condition prescribed by the user as the inflow value is required to find the sectional aerodynamic loads.
- Flap calculation is initiated based on the user's command. If the user does not require flap to be included in the calculations, flap angle is assumed as zero and the code proceeds to further calculations.
- Sectional loads are estimated and stored as an array. These loads include airfoil lift, drag and pitching moment.
- The stored sectional loads are transformed to TH reference frame and integrated using Gauss-Quadrature method.
- The net TH frame loads are then transformed to FH frame. Flap calculations is performed based on the user's command.
- The same process is repeated in an azimuthal loop for all rotor components together. The loads are stored, and the calculations are stopped for each component once the inflow and flap values meet the predefined convergence criteria for that component.
- Once all the required parameters converge, the individual blade loads of each component are then transferred to the HFNR frame of that component where the net hub loads are calculated.
- The obtained net hub load values of individual components are all transferred to CG frame and stored in an array for further calculations. Refer Figure-4.2

Table 1: Convergence study for Gaussian quadrature

	$F_X$	$F_Y$	$F_Z$	$M_X$	$M_Y$	$M_Z$
10	0	-1200.990004	11218.08118	-41.5595	-53336.85452	-5494
20	0	-1826.835142	19196.19679	-41.56008	-77370.9226	-6805
30	0	-1826.835142	19196.19679	-41.56008	-77370.9226	-6805
40	0	-1826.835142	19196.19679	-41.56008	-77370.9226	-6805

#### 4.4.2 Non-Rotating Component Loads

- If fuselage components were entered in the input file, the fuselage drag is estimated using quasi-steady theory for each such component. The estimated load is transferred to CG frame.
- If stabilizer components were entered in the input file, the stabilizer loads are estimated using quasi-steady theory for each such component and transferred to CG frame (see fig 4.1).

#### 4.4.3 Trim Analysis

- The required vehicle and component parameters are retrieved from the respective class objects stored in Global File. The input guess for the trim states is taken from the user.
- Net loads at CG are estimated for all rotors and non-rotating components.
- Using the flight dynamic equations, the acceleration at CG is estimated.
- Newton-Raphson algorithm is used to obtain the trim states with the acceptable tolerance to the acceleration values (see fig 4.2).

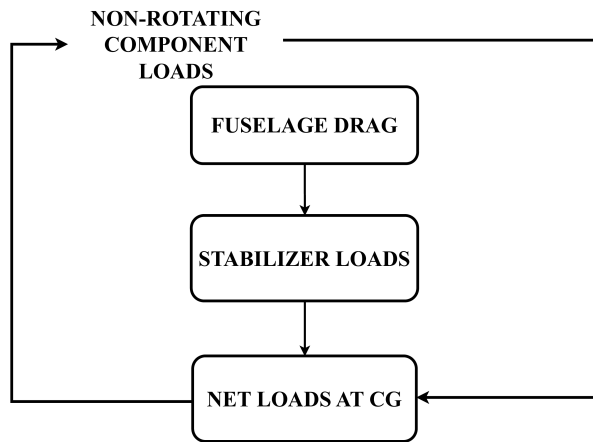


Figure 4.1: Non-rotating components load calculation

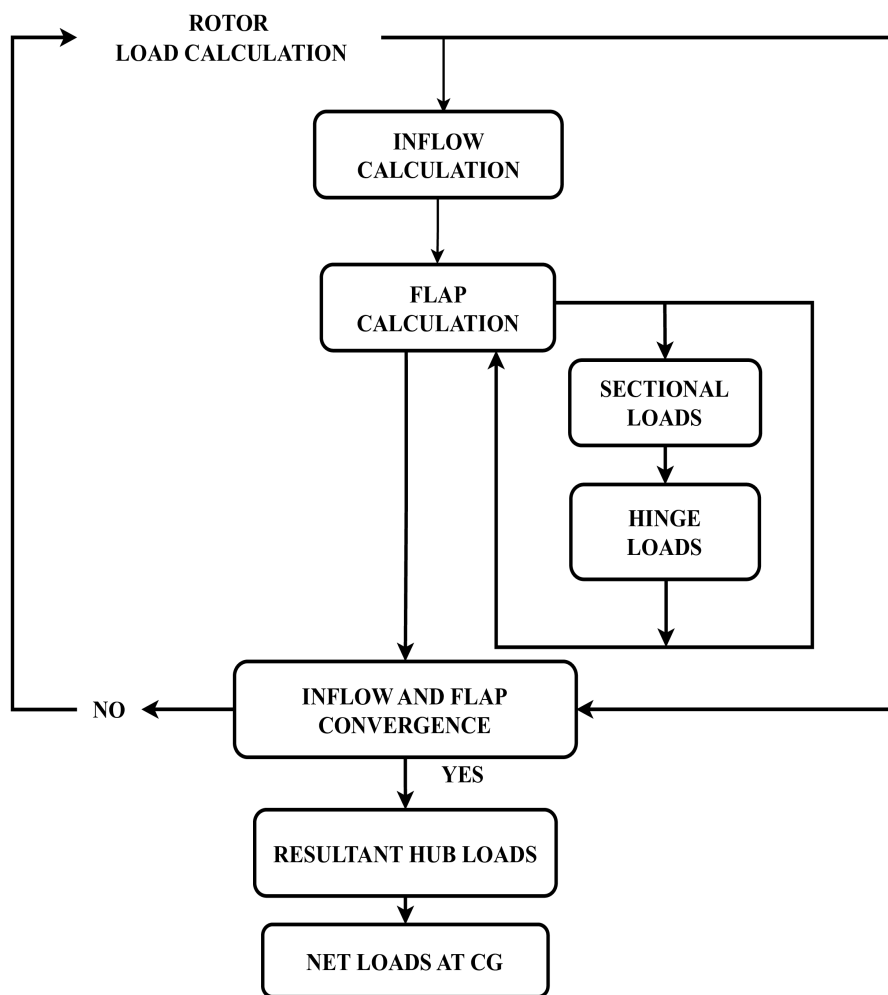


Figure 4.2: Rotor load calculation

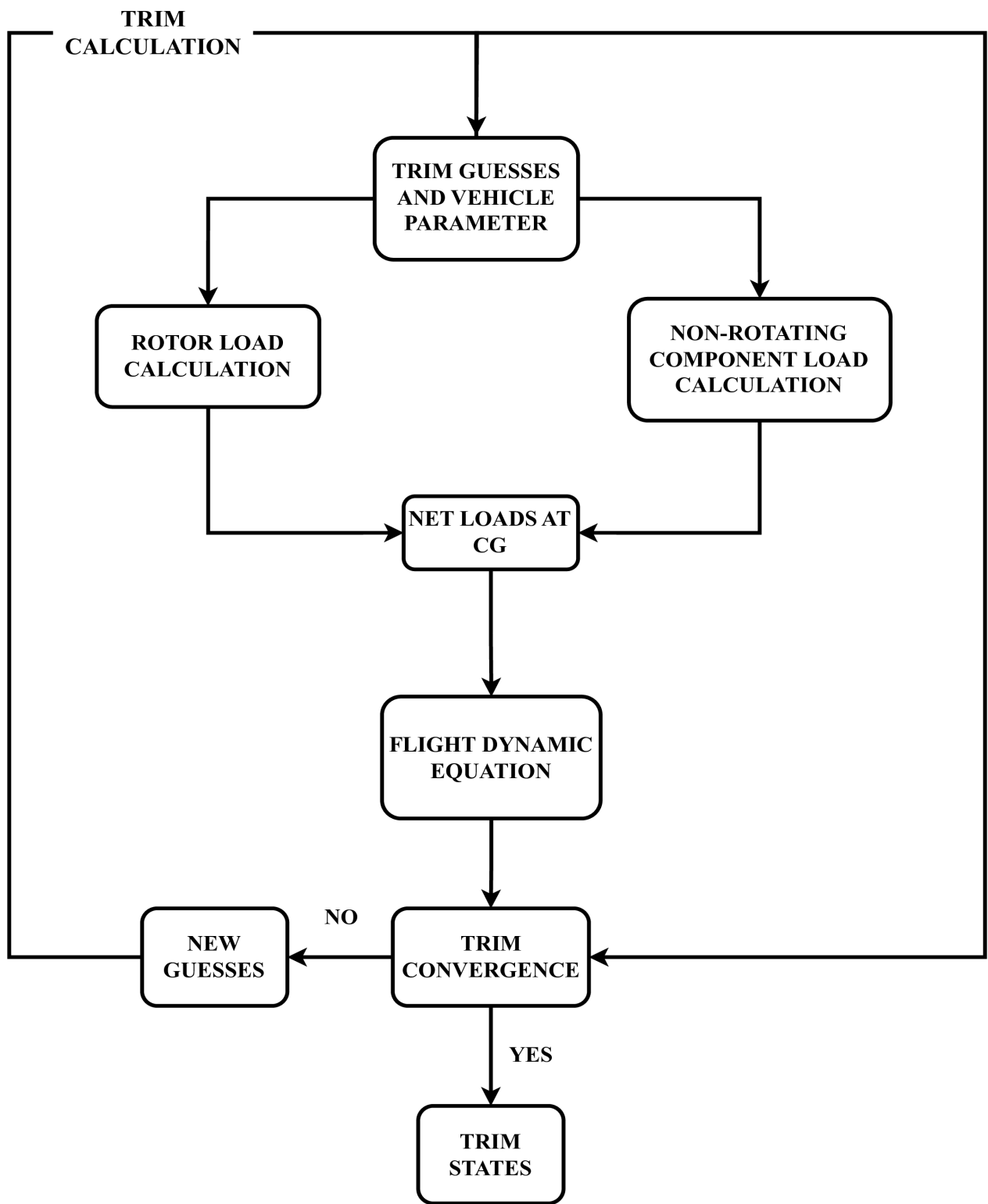


Figure 4.3: Trim calculation

## 5. Solution Methodology

Trim is the primary flight dynamic analysis. It is performed to obtain the control parameters for which the aircraft will reach equilibrium for the given flight condition. Trim analysis is a prerequisite for the analysis of stability and control response. This chapter describes the solution procedure to evaluate trim states of the given configuration for the given flight conditions. In the first section, the set of equations used for the trim of conventional and coaxial configuration is presented. In the second section, the generalized trim procedure is explained. In the final section, the obtained trim results are discussed.

### 5.1 Mathematical Formulation for Trim

Trim is the state of force and moment balance. Trim states are desirable during cruise and other maneuvers as it increases the aircraft performance and helps maintain stability, improves pilot and passenger comfort etc. Therefore, trim analysis is an essential part of flight dynamic models. The trim equations are solved to obtain the trim parameters.

$$\dot{u} = -(wq - vr) + \frac{X}{m_h} - g\sin\theta \quad (5.1.1)$$

$$\dot{v} = -(ur - wp) + \frac{Y}{m_h} + g\cos\theta\sin\phi \quad (5.1.2)$$

$$\dot{w} = -(vp - uq) + \frac{Z}{m_h} + g\cos\theta\cos\phi \quad (5.1.3)$$

$$\dot{p} = \frac{1}{I_{xx}} (I_{yy} - I_{zz})rq + I_{xz}(\dot{r} + pq) + L \quad (5.1.4)$$

$$\dot{q} = \frac{1}{I_{yy}} (I_{zz} - I_{xx})rp + I_{xz}(r^2 - p^2) + M \quad (5.1.5)$$

$$\dot{r} = \frac{1}{I_{zz}} (I_{xx} - I_{yy})pq + I_{xz}(\dot{p} - rq) + N \quad (5.1.6)$$

While the equations discussed thus far are enough for the trim analysis of conventional helicopter configurations, trim analysis of coaxial helicopters is not straightforward. In coaxial helicopters, the trim parameters include

$$X = [\theta_0, \theta_{diff}, \theta_{1c}, \theta_{1s}, \theta, \phi, \theta_{1cdiff}, \theta_{1sdiff}]^T \quad (5.1.7)$$

Note that there are eight control parameters but only six flight dynamic equations. Therefore, additional equations are required to make the system of equations consistent. To achieve this, the longitudinal differential is set to zero and the lateral differential is set to limit the lift offset (LOS) value. This is done so that the rotors are working in non-stall working condition [26]. The limiting lift offset equation is given by:

$$LOS = \frac{\Delta M_x}{TR} \quad (5.1.8)$$

Here,  $\Delta M_x$  is the differential rolling moment, T is the total rotor lift and R is the radius of the rotor. According to [27], the value of LOS is set to vary with the flight speed according to the relation:

$$LOS = 0.0002V^2 \quad (5.1.9)$$

$$\Delta LOS = 0.0002V_f^2 - \frac{\Delta M_x}{TR} \quad (5.1.10)$$

$\Delta LOS$  is set this way so that no lateral offset is required during hover. This equation is added to the six flight dynamic equations. With the elimination of longitudinal lift offset and addition of LOS equation, the system is consistent with seven equations in seven unknowns.

## 5.2 Generalized Trim Procedure

The configuration of the vehicle is an important consideration in developing a trim strategy as it determines the number of control parameters. In this section, a generalized procedure is proposed for the trim analysis of conventional and coaxial helicopters.

1. The vehicle configuration data and type are read from the input file. Component class objects are created. The atmosphere module is used to estimate atmospheric properties.
2. Reference frames are created for all components. The creation of reference frames for the clockwise rotor and the counterclockwise rotor were explained in detail in Chapter 3.
3. Initial trim guesses as entered by the users are utilized to start the trim algorithm. If the configuration is conventional, the trim parameters are treated as  $X_1$ . If the configuration is coaxial, the trim parameters are treated as  $X_2$ . Based on the configuration, the control angles and component class objects

are passed to the rotor load calculation module in Rotor Loads File to obtain the rotor loads at CG frame.

4. Load calculation for non-rotating components is done sequentially. Firstly, loads for all fuselage components, then the stabilizer components. Finally, all the component loads including rotors and non-rotating components are added to obtain the net loads at CG.
5. If the configuration is conventional, these loads are directly substituted in the trim equations to obtain the six accelerations. If the configuration is coaxial, in addition to the six accelerations, the LOS relation is also used and treated in the same way as the accelerations.
6. The obtained accelerations are checked for convergence with a preset value of tolerance. If the accelerations are within the tolerance, the Newton-Raphson iteration is terminated as the current control parameters are the required trim states. If not, the Newton-Raphson algorithm proceeds to the Jacobian calculations.
7. The obtained accelerations are the reference acceleration values for the current iteration of Newton-Raphson algorithm. The rate of change of accelerations with small perturbations of individual trim parameters are obtained. This is used to construct the Jacobian matrix.
8. The obtained Jacobian matrix is then inverted and utilized in the Newton-Raphson algorithm to estimate the new trim parameters. These new parameters are used to start the next iteration of the same procedure from step 3.

$$X_1 = \{\theta_0, \theta_{1c}, \theta_{1s}, \theta_{tr}, \theta, \phi\} \quad (5.2.1)$$

$$X_2 = \{\theta_0, \theta_{0diff}, \theta_{1c}, \theta_{1s}, \theta_{1cdiff}, \theta_{1sdiff}, \theta, \phi\} \quad (5.2.2)$$

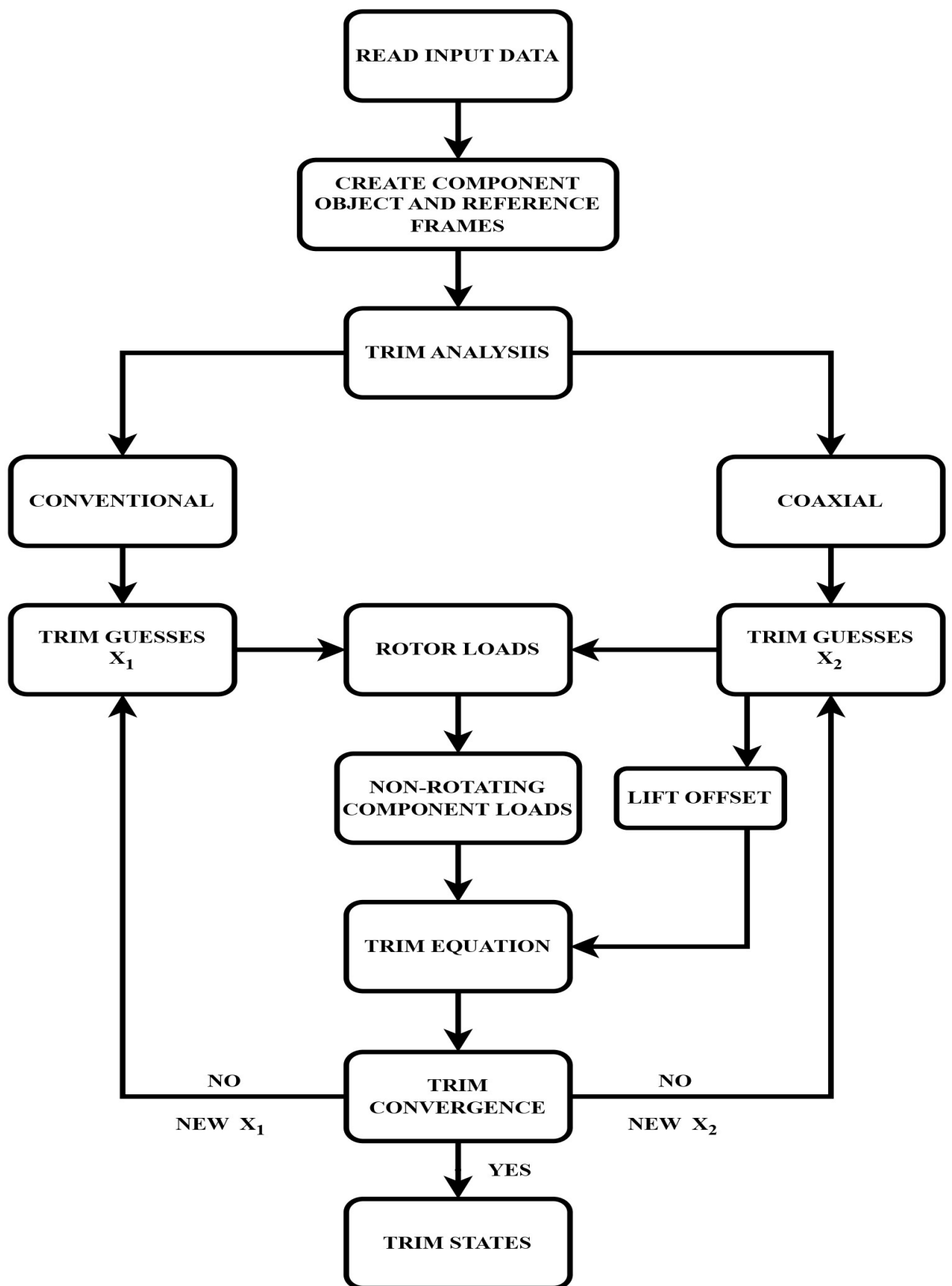


Figure 5.1: Generalized Trim Procedure

## 6. Results

This chapter displays the significant results obtained in this work so far. This chapter contains two sections. The first section focuses on the flap results of Conventional configuration rotor. In the second section, the trim results for Conventional Helicopter Configuration is discussed in detail.

### 6.1 Inflow for Conventional Configuration

In this section, Drees inflow variation is plotted against the azimuthal position. While the inflow ratio values cannot be validated as such, the expected trend based on the physics of the problem is observed.

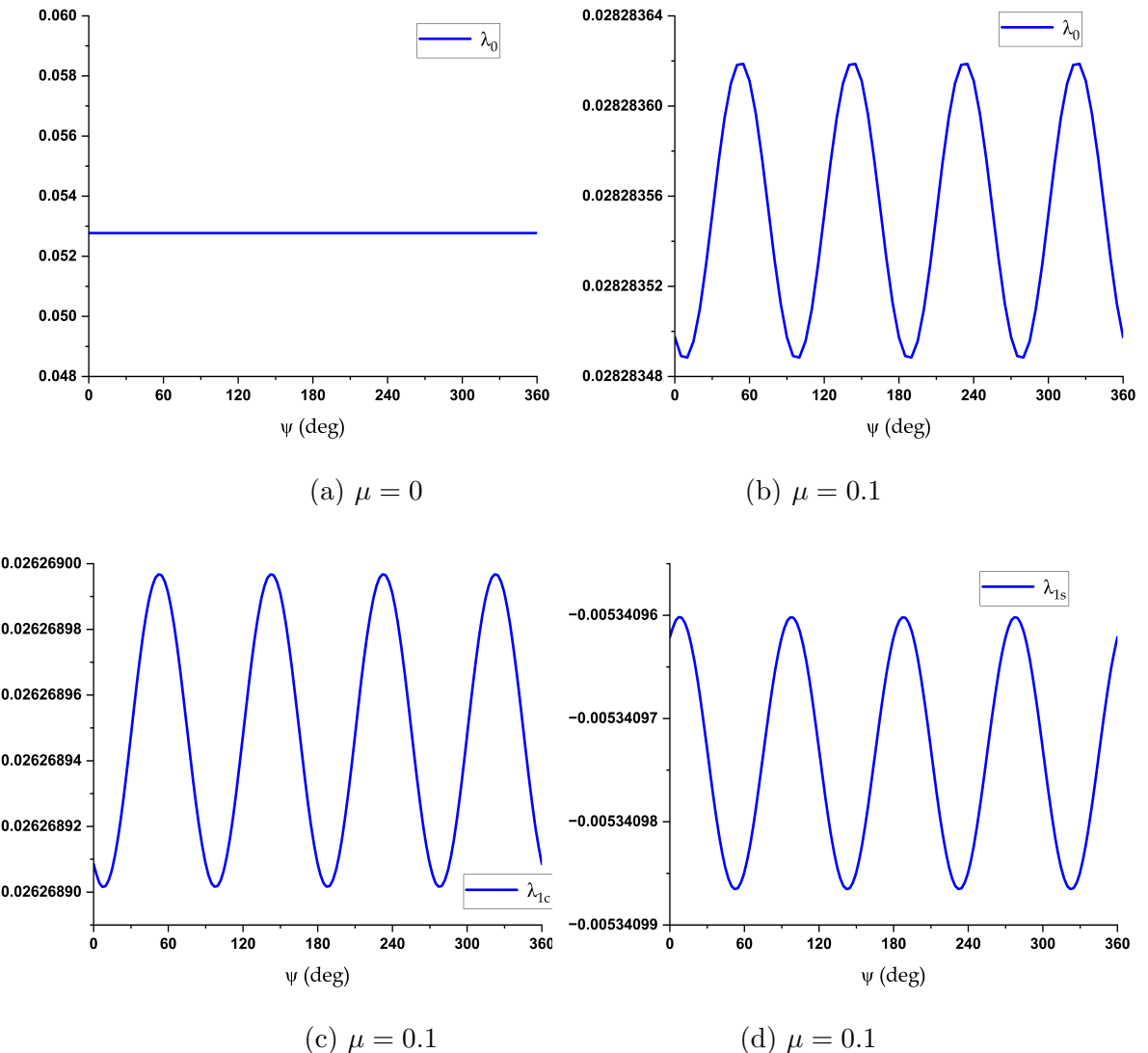


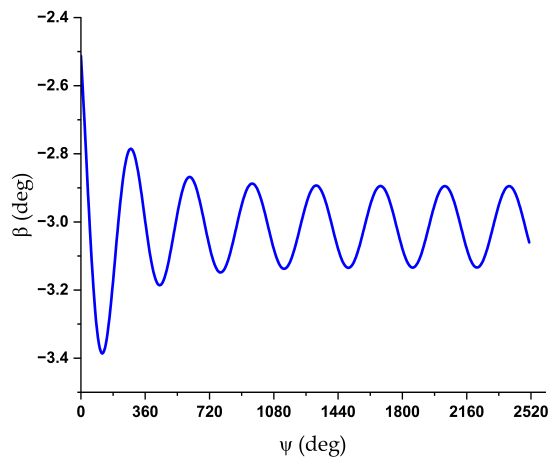
Figure 6.1: Inflow results for Conventional Configuration

## 6.2 Flap for Conventional Configuration

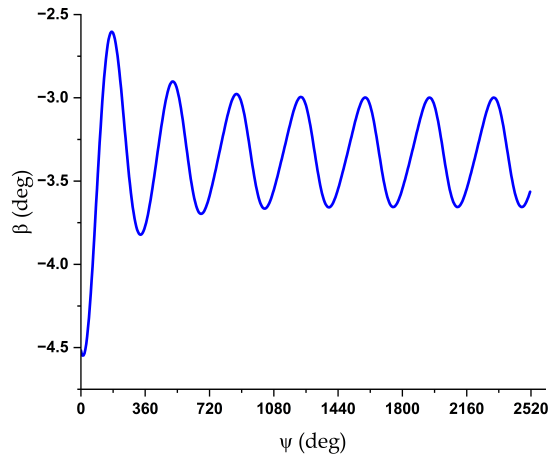
The flapping motion of the blades is a very important consideration in the analysis of rotors as this phenomenon affects the aerodynamic loads and hence the rotor performance directly. fig 6.2 displays the convergence of flap angle, angular velocity and acceleration. With good initial conditions, the flap parameters converged within four to six full revolutions and when the initial conditions were particularly bad, the values may converge after 10 to 12 revolutions or even diverge. The results presented below are for the Conventional configuration main rotor, whose parameters are tabulated in table 2. The inflow model was selected to be dynamic inflow.

### 6.2.1 Observations

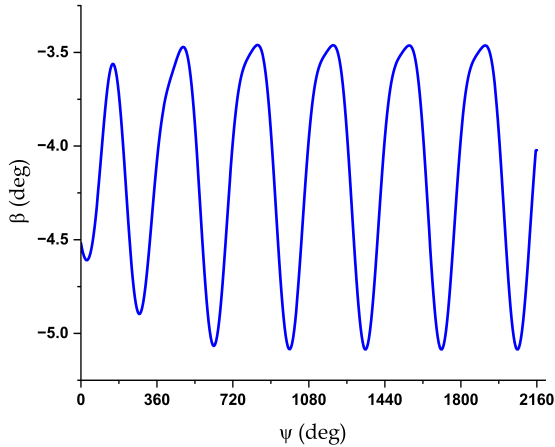
- It was observed that the values converged in just three full revolutions.
- One per rev flapping motion is observed as expected.
- Although the data cannot be validated as such, this result gives us some confidence moving forward.
- It was observed that the inclusion of flap calculation increased the time to obtain rotor loads to over double the amount. This is because of the higher number of calculations than the case without flap and also the higher number of full revolutions required to attain both inflow and flap convergence.



(a)  $\mu = 0$



(b)  $\mu = 0.1$



(c)  $\mu = 0.2$

Figure 6.2: Flap Convergence

### 6.3 Trim for Conventional Helicopter Configuration

The Conventional Helicopter configuration is one with a main rotor, a tail rotor, a fuselage, a horizontal and a vertical stabilizer. Conventional configuration is used for the validation of the trim module as was done by Sakthivel T [13]. The vehicle parameters can be found in Table-2. Before further discussion, it must be made clear that the reference values from [13] include the effects of flap and also that both the rotors are modelled with dynamic inflow. Additionally, the sectional loads are modelled using modified ONERA model which includes the effect of dynamic stall.

The obtained trim results are displayed in fig 6.3. Our Model(low fidelity) displays the case where the main rotor is modelled with Drees inflow and the tail rotor is modelled only by providing thrust. Our Model(high fidelity) displays the case where the main rotor is modelled with Drees inflow and the tail rotor is modelled with dynamic inflow.

#### 6.3.1 Observations

- As can be observed overall from fig 6.3, current study data matches with the low fidelity values from [13].
- Since the results are consistent with low fidelity values, achieving high fidelity values is not very challenging.
- High fidelity values will eventually be achieved by testing Flap and dynamic inflow usage.
- The total trim values are shown in the table 3.

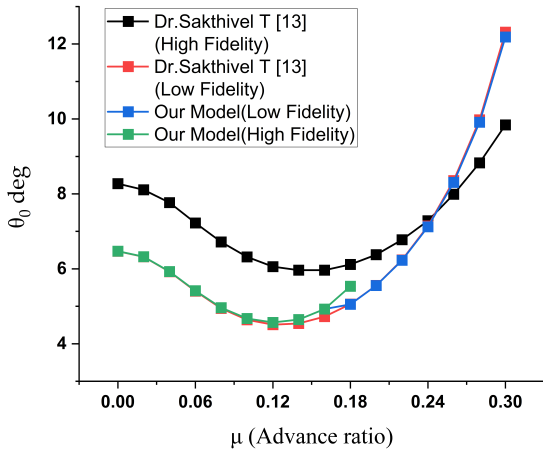
### 6.3.2 Conventional Configuration Data

Table 2: Conventional Configuration for Trim Analysis

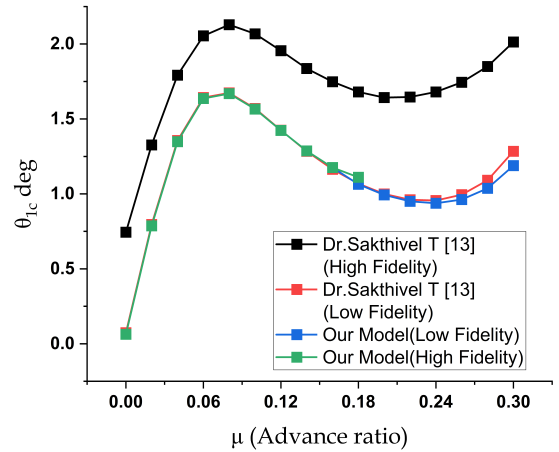
Parameter	Unit	Value	
		Main rotor	Tail rotor
Radius	m	6.6	1.275
Rotor speed	rad/s	32.88	163.772
No. of. blades	-	4	4
Lift curve slope	-	5.73	5.73
Chord	m	0.5	0.19
Twist	deg	-12	-12
Mass per unit length	kg/m	11.21	-
Flap frequency	-	1.09	-
Hinge offset	m	0.807	0.147
Position of Hub from CG	m	0.05; 0.0; -1.6	-7.9; 0.0; -2.0
Fuselage			
Mass	kg	4500	
Mass moment of inertia $I_{xx}, I_{yy}, I_{zz}$	$\text{kg} \cdot \text{m}^2$	5000; 20000; 16700	
Product of inertia $I_{xz}$	$\text{kg} \cdot \text{m}^2$	3700	
Fuselage Flat area	$\text{m}^2$	1.8	
Horizontal tail			
Area	$\text{m}^2$	1.326	1.2036
Position from CG	m	-7.325; 0; -0.535	-7.313; 0; -0.452
Initial setting angle	deg	1.5	2

Table 3: Trim Results for Conventional Configuration

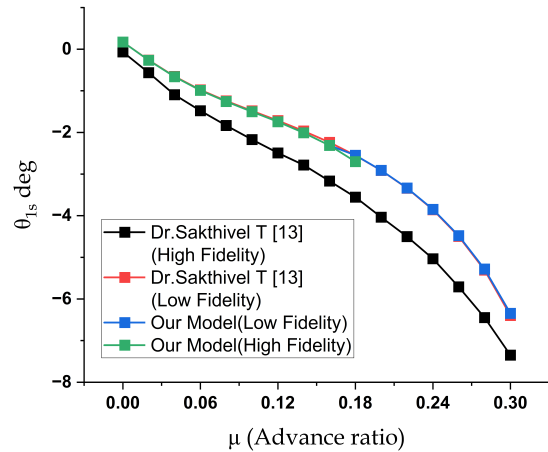
$\mu$	$\theta_0$ (deg)	$\theta_{1c}$ (deg)	$\theta_{1s}$ (deg)	TR Thrust(N)	$\theta$ (deg)	$\phi$ (deg)
0	6.47	0.06	0.17	2746.32	-0.11	-3.52
0.02	6.32	0.78	-0.26	2679.12	-0.17	-3.07
0.04	5.92	1.34	-0.66	2491.88	-0.28	-2.56
0.06	5.41	1.63	-0.98	2245.35	-0.45	-2.12
0.08	4.96	1.66	-1.25	2017.18	-0.69	-1.84
0.1	4.67	1.56	-1.50	1851.77	-1.01	-1.72
0.12	4.56	1.42	-1.74	1755.10	-1.40	-1.72
0.14	4.64	1.28	-2.00	1721.44	-1.91	-1.82
0.16	4.92	1.17	-2.31	1745.38	-2.57	-2.01
0.18	5.05	1.06	-2.54	1826.53	-2.74	-2.11
0.2	5.55	0.99	-2.90	1969.11	-3.40	-2.38
0.22	6.22	0.95	-3.33	2177.86	-4.16	-2.71
0.24	7.12	0.93	-3.84	2466.93	-5.05548	-3.11
0.26	8.30	0.96	-4.47	2862.07	-6.15182	-3.57
0.28	9.91	1.03	-5.27	3407.31	-7.56	-4.08
0.3	12.18	1.18	-6.34	4192.74	-9.54	-4.58



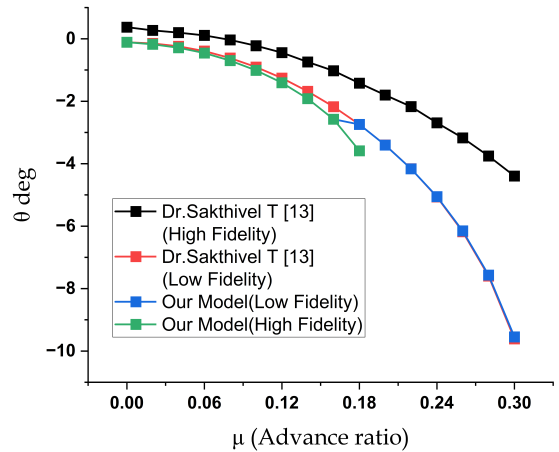
(a) Collective



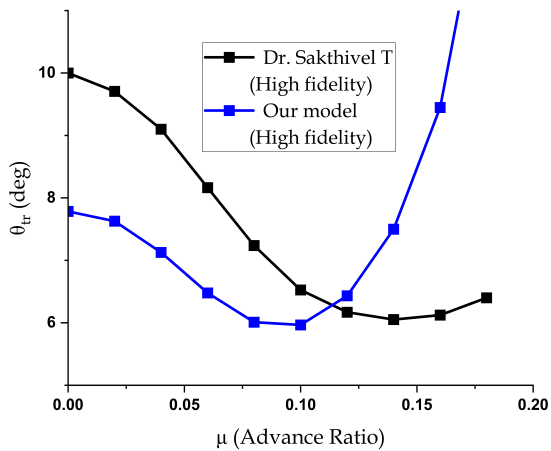
(b) Lateral cyclic



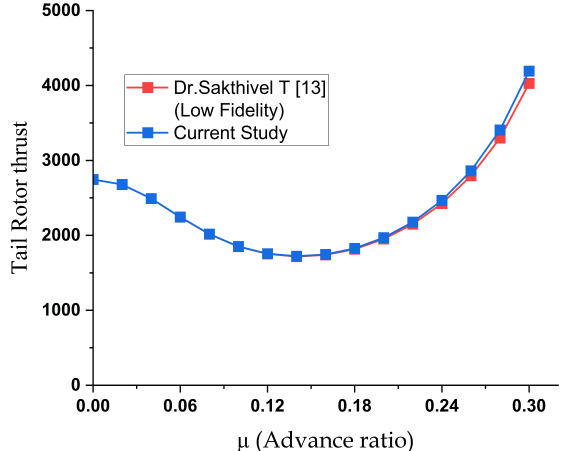
(c) Longitudinal cyclic



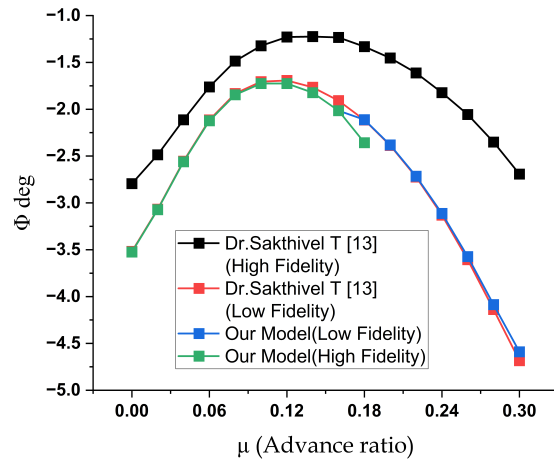
(d) Pitch



(e) TR collective



(f) TR thrust



(g) Roll

Figure 6.3: Trim results for Conventional Configuration

## 6.4 Trim for Coaxial Configuration

The trim results of coaxial configuration. Table 4 shows the the trim control parameters in hover.

Table 4: Coaxial Trim for  $\mu=0$  (Hover)

Trim Parameters	Current Study	Flight Data [28]
$\theta_0$ (deg)	7.50	14.0
$\theta_{1c}$ (deg)	0	0
$\theta_{1s}$ (deg)	0	0
$\theta_0$ lower rotor (deg)	7.50	14.0
$\theta_{1c}$ lower rotor (deg)	0	0
$\theta$ (deg)	0	0
$\phi$ (deg)	0	0

### 6.4.1 Coaxial Configuration Data

Table 5: Coaxial Configuration for Trim Analysis

Parameter	Unit	Value
Coaxial		
Radius	m	5.49
Rotor speed	rad/s	35 / 35.9
No. of. blades	-	6
Rotor solidity	-	0.127
Pre-twist	deg	-10
Twist	deg	3
Shaft tilt	deg	3
Shaft spacing	m	0.77
Taper ratio		0.5
Flap frequency	-	1.4
Spring stiffness	N.m/rad	220500
Lower rotor position	m	0.0; 0.0; -0.89
Lock number		5.41
Fuselage		
Mass	kg	5500
Flap moment of inertia	$\text{kg} \cdot \text{m}^2$	450
		Horizontal stabilizer      Vertical stabilizer
Area	$\text{m}^2$	5.57      2.79
Position from CG	m	-6.80; 0; 0.20      -6.80; 0; -0.50

## 7. Conclusion

Developing a generic and modular rotorcraft flight dynamic model is a challenging and rewarding endeavor. The primary conclusions based on the work and the presented results are as follows.

- From the literature survey, it was evident that many models exist with various advantages. We attempted to bring together as many advantages as possible in one program, while avoiding major pitfalls.
- The modelling of components were done by choosing mathematical models with reasonable accuracy and lower computational requirements. Rotor modelling in particular, was a difficult task due to runtime and convergence issues regarding inflow and flap calculations.
- For Conventional configuration, the program does yields satisfying results at low to medium forward speeds. The Coaxial configuration yields proper results at hover. The program does not yield satisfying results in high forward speeds.

The primary objectives of the current work, modularity and genericity, have been successfully demonstrated through the results presented in this report. While the accuracy can be improved, the results presented in this report meet the expectations for the considered simple cases.

## 8. Future Scope

The current work offers a broad scope of improvement and utility. It can be extended to include various features and also to improve the accuracy of the results obtained. Some of the conceivable and necessary future improvements are listed below.

- Computation time can be reduced by incorporating quick and efficient ways of storing and handling reference frame data such as DCM, loads etc.
- Incorporation of the effects of lag and torsion dynamics increase the accuracy of the model.
- Elastic and aeroelastic formulations can also be included to model the physics of rotors accurately.
- Extend the flight dynamic model to support unconventional designs such as tiltrotors. This requires a generalised mapping between the trim equations and control parameters.
- Extend the model to include stability analysis and the simulation of control response for given control inputs and flight conditions.
- Incorporate analysis modules such as whirl tower tests that will aid in the design of rotors for various applications.
- Develop a Graphical User Interface (GUI) for dynamic interaction between the user and the program.

## References

- [1] C. Venkatesan, *Fundamentals of helicopter dynamics*. CRC Press, 2014.
- [2] A. Filippone, *Flight performance of fixed and rotary wing aircraft*. Elsevier, 2006.
- [3] G. J. Leishman, *Principles of helicopter aerodynamics with CD extra*. Cambridge university press, 2006.
- [4] M. D. Maisel, *The history of the XV-15 tilt rotor research aircraft: from concept to flight*. No. 17, National Aeronautics and Space Administration, Office of Policy and Plans . . . , 2000.
- [5] T. Theodorsen, “General theory of aerodynamic instability and the mechanism of flutter,” technical report, nasa tr -496,.
- [6] J. M. Greenberg, “Airfoil in sinusoidal motion in a pulsating stream,” tech. rep., 1947.
- [7] J. M. Greenberg, “Some considerations on an airfoil in an oscillating stream,” tech. rep., 1947.
- [8] R. G. Loewy, “A two-dimensional approximation to the unsteady aerodynamics of rotary wings,” *Journal of the Aeronautical Sciences*, vol. 24, no. 2, pp. 81–92, 1957.
- [9] D. Petot, “Differential equation modeling of dynamic stall,” *La Recherche Aerospatiale(English Edition)*, no. 5, pp. 59–72, 1989.
- [10] V. Laxman and C. Venkatesan, “Chaotic response of an airfoil due to aeroelastic coupling and dynamic stall,” *AIAA journal*, vol. 45, no. 1, pp. 271–280, 2007.
- [11] A. Datta, M. Nixon, and I. Chopra, “Review of rotor loads prediction with the emergence of rotorcraft cfd,” *Journal of the American Helicopter Society*, vol. 52, no. 4, pp. 287–317, 2007.
- [12] D. L. Kunz, “Survey and comparison of engineering beam theories for helicopter rotor blades,” *Journal of Aircraft*, vol. 31, no. 3, pp. 473–479, 1994.

- [13] T. Sakthivel, “Flight dynamic analysis of a helicopter in steady maneuver and estimation of handling quality parameters,” PhD. thesis, Dept. of Aerospace Eng., IIT - Kanpur.
- [14] R. T. Chen, “A survey of non-uniform inflow models for rotorcraft flight dynamics and control applications,” in *European Rotorcraft Forum*, no. A-89220, 1989.
- [15] K. Krothapalli, J. Prasad, and D. Peters, “Helicopter rotor dynamic inflow modeling for maneuvering flight,” *Journal of the American Helicopter Society*, vol. 46, pp. 129–139, 04 2001.
- [16] R. P. Coleman, A. M. Feingold, and C. W. Stempin, “Evaluation of the induced-velocity field of an idealized helicopter rotor,” tech. rep., National Aeronautics and Space Administration Hampton Va Langley Research Center, 1945.
- [17] K. Mangler and H. B. Squire, “The induced velocity field of a rotor,” 1950.
- [18] D. A. Peters, “How dynamic inflow survives in the competitive world of rotorcraft aerodynamics,” *Journal of the American Helicopter Society*, vol. 54, no. 1, pp. 11001–11001, 2009.
- [19] J. C. Wilson and R. E. Mineck, “Wind tunnel investigation of helicopter rotor wake effects on three helicopter fuselage models,” tech. rep., 1974.
- [20] J. Kim and T. Tsuchiya, “Openvsp based aerodynamic design optimization toll building method and its application to tailless uav,” in *33rd Congress of the International Council of the Aeronautical Science, Stockholm, Sweden*, 2022.
- [21] V. Laxman, J.-H. Lim, S.-J. Shin, K.-H. Ko, and S.-N. Jung, “Power and trim estimation for helicopter sizing and performance analysis,” *International Journal of Aeronautical and Space Sciences*, vol. 12, no. 2, pp. 156–162, 2011.
- [22] S. W. Ferguson, “A mathematical model for real time flight simulation of a generic tilt-rotor aircraft,” *NASA CR-166536*, vol. 1, 1988.
- [23] C. Quiding, C. Ivler, and M. Tischler, “Genhel s-76c model correlation using flight test identified models,” in *ANNUAL FORUM PROCEEDINGS-AMERICAN HELICOPTER SOCIETY*, vol. 64, p. 922, AMERICAN HELICOPTER SOCIETY, INC, 2008.
- [24] C. Fegely, O. Juhasz, H. Xin, and M. B. Tischler, “Flight dynamics and control modeling with system identification validation of the sikorsky x2 technology™

demonstrator,” in *American Helicopter Society 72nd Annual Forum, West Palm Beach, FL*, 2016.

- [25] D. M. Pitt, *Rotor dynamic inflow derivatives and time constants from various inflow models*. Washington University in St. Louis, 1980.
- [26] Y. Su, Z. Wang, and Y. Cao, “A hybrid trim strategy for coaxial compound helicopter,” *Proceedings of the Institution of Mechanical Engineers, Part G: Journal of Aerospace Engineering*, vol. 237, no. 2, pp. 452–466, 2023.
- [27] K. M. Ferguson, *Towards a better understanding of the flight mechanics of compound helicopter configurations*. PhD thesis, University of Glasgow, 2015.
- [28] Y. Yuan, R. Chen, and P. Li, “Trim investigation for coaxial rigid rotor helicopters using an improved aerodynamic interference model,” *Aerospace Science and Technology*, vol. 85, pp. 293–304, 2019.
- [29] R. Chen, Y. Yuan, and D. Thomson, “A review of mathematical modelling techniques for advanced rotorcraft configurations,” *Progress in Aerospace Sciences*, vol. 120, p. 100681, 2021.
- [30] R. B. Gray, “A review of rotor induced velocity field theory,” 1954.
- [31] H. Glauert, “A general theory of the autogyro,” tech. rep., HM Stationery Office, 1926.
- [32] L. K. Loftin Jr, “Airfoil section characteristics at high angles of attack,” tech. rep., 1954.
- [33] R. L. Barrie, *Time domain validation of the Sikorsky General Helicopter (Gen-Hel) Flight Dynamics Simulation Model for the UH-60L Wide Chord Blade modification*. PhD thesis, Monterey, California: Naval Postgraduate School, 1999.
- [34] W. Qiuqiu, G. Shijun, L. Hao, and D. Wei, “Nonlinear dynamics of a flapping rotary wing: Modeling and optimal wing kinematic analysis,” *Chinese Journal of Aeronautics*, vol. 31, no. 5, pp. 1041–1052, 2018.
- [35] W. Z. Stepniewski and C. Keys, *Rotary-wing aerodynamics*. Courier Corporation, 1984.
- [36] V. Laxman, “Formulation of a computational aeroelastic model for the prediction of trim and response of a helicopter rotor system in forward flight, ph.”